

**A NOVEL OPTO-ELECTRO-MECHANICAL TACTILE  
SENSOR FOR BREAST CANCER IMAGING**

**A THESIS SUBMITTED TO  
THE GRADUATE SCHOOL OF ENGINEERING  
OF  
KOÇ UNIVERSITY**

**BY**

**MEHMET AYYILDIZ**

**IN PARTIAL FULFILLMENT OF THE REQUIREMENTS  
FOR  
THE DEGREE OF MASTER OF SCIENCE  
IN  
MECHANICAL ENGINEERING**

**JULY 2011**

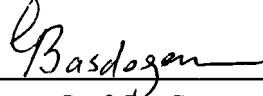
Koç University  
Graduate School of Sciences and Engineering

This is to certify that I have examined this copy of a master's thesis by

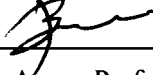
Mehmet Ayyıldız

and have found that it is complete and satisfactory in all respects,  
and that any and all revisions required by the final  
examining committee has been made.

Committee Members:



Assoc. Prof. Dr. Çağatay Başdoğan (Advisor)



Assoc. Prof. Dr. Burak Güçlü



Asst. Prof. Dr. Demircan Canadıncı

Date:

21 / 07 / 2011

# ACKNOWLEDGEMENTS

It is a pleasure to thank those who made this thesis possible, Assoc. Prof. Dr. Çağatay Başdoğan and Assoc. Prof. Dr. Burak Güçlü. I owe my deepest gratitude to them for their continuous support, guidance and encouragement. I warmly thank Mustafa Zahid Yıldız, Can Gökğöl, Umut Özcan and Bektaş Baybora Baran for sharing their knowledge and experience with me. Their friendly help and our discussions about my work have been very helpful for this study.

I would like to thank Asst. Prof. Dr. Demircan Canadınç and Assoc. Prof. Dr. İpek Başdoğan for their dedication and excellence in teaching. They provided me a better understanding of my research with their graduate courses.

I am also grateful to the graduate school of science officers: Emine Büyükdurmuş and Gülçin Sincan. They have been quite problem solvers and troubleshooters with their remarkable efforts and helpful suggestions.

I thank Composite Materials Manufacturing Laboratory (CMML) for their collaboration in preparing silicon samples.

The great friendship, shared quality times and generous support from Utku Boz, Serkan Külâh, Mustafa R. Haboğlu, Talha Akyol, Barış Çağlar, Mehmet Akif Yalçınkaya, Bekir Yenilmez, Ayşe Küçükyılmaz, Emre Ölçeroğlu, Yunus Emre Has, Arda Aytekin, Berkay Yarpuzlu and Uğur Arıdoğan are appreciated.

Most special thanks go to Fatma Virdil for her outstanding company, friendship, support and understanding.

I gratefully acknowledge TUBITAK (Scientific and Technological Research Council of Turkey) Graduate Scholarship Programme (Code 2210) for their financial support.

Finally, I would like to thank my parents: Hüseyin and Seyide Ayyıldız; my sister, Meltem Ayyıldız for their precious support in every stage of my life.

# TABLE OF CONTENTS

ACKNOWLEDGEMENTS.....	i
TABLE OF CONTENTS.....	ii
ABSTRACT.....	iv
ÖZET .....	v
LIST OF SYMBOLS .....	vi
LIST OF ABBREVIATIONS.....	vii
LIST OF FIGURES .....	viii
LIST OF TABLES.....	x
1. INTRODUCTION .....	1
1.1 Breast Cancer .....	1
1.2 Breast Cancer Imaging .....	3
1.2.1 Conventional modalities.....	3
1.2.2 Tactile imaging.....	7
1.2.3 Our approach: Opto-Electro-Mechanical Tactile Imaging .....	9
2. METHODS AND MATERIALS.....	10
2.1 Design of the Tactile Sensor .....	10
2.2 Data Acquisition.....	12
2.3 Calibration.....	13
2.4 Data Processing .....	14
3. EXPERIMENTS.....	17
3.1 Compression Experiments .....	19
3.2 Performance Evaluation of our TI system .....	20

3.3	Manual Palpation Experiments .....	23
3.4	Performance Evaluation for the Manual Palpation Experiments .....	24
4.	RESULTS .....	25
4.1	TI System .....	25
4.2	Manual Palpation Experiments .....	28
4.3	Comparison of the TI system and the Manual Palpation .....	30
5.	DISCUSSION .....	32
5.1	Discussion of our Work .....	32
5.1.1	TI system .....	32
5.1.2	Silicon samples.....	33
5.1.3	Comparison of the TI system and the Manual Palpation .....	33
5.2	Discussion with the Other Works .....	34
5.2.1	Comparison with the conventional breast cancer imaging modalities .	34
5.2.2	Comparison with the other TI systems.....	35
6.	CONCLUSION AND FUTURE WORK .....	37
	REFERENCES .....	39

## ABSTRACT

We developed a compact Tactile Imaging (TI) system in order to guide the clinician or the self-user for non-invasive detection of breast lumps. Our TI system consists of  $10 \times 10$  infrared emitter-detector sensors, a silicon-rubber elastic pad, and a contoured tactile interface ( $25 \times 21$  moving pins) for palpating breast tissue. The proposed TI system is more cost-effective than the conventional imaging techniques such as mammography, MRI, and ultrasonography. Furthermore, it has no side effects during or after the breast examination and can be used by women who are pregnant or breastfeeding. Compared to the other TI systems utilizing capacitive or piezo-based sensing technologies, the proposed system conforms to the palpable object, which results in distributed force sensing and leads to higher spatial resolution. In order to evaluate the performance of the proposed TI system, tissue-like cylindrical silicon samples containing tumor-like inclusions were prepared first. Then, compression experiments were performed with the TI system to measure its sensitivity and specificity in detecting those inclusions. Based on the experiments performed with 11 inclusions, having 2 different sizes and 2 different stiffnesses, located at 3 different depths, our TI system showed an average sensitivity of  $90.82 \pm 8.08\%$ , an average specificity of  $89.80 \pm 12.66\%$ . Finally, manual palpation experiments were performed with 12 human subjects on the same silicon samples and the results were compared to that of the TI system. The performance of the TI system was significantly better than that of the human subjects in detecting deep inclusions while the human subjects performed slightly better in detecting shallow inclusions close to the contact surface.

## ÖZET

Meme tümörlerinin non-invazif olarak teşhisinde klinisyenlere ve ev kullanıcılarına yol gösterecek kompakt bir dokunsal sensör geliştirdik. Bu sensör 10 x 10 kızılötesi ışık yayıcı-alıcı ikililerinden, bir elastik silikon katmandan ve meme dokusunu muayene etmek için memeyi çevreleyen bir dokunmatik arayüzden (25x21 hareketli pim) oluşmaktadır. Yeni tasarımımızın maliyeti mamografi, MRI ve ultrasonografi gibi klasik yöntemlere göre daha düşüktür. Ayrıca bu yöntem meme muayenesinden önce veya sonra herhangi bir yan etkiye sebep olmamakta, hamile veya bebek emziren bayanlara uygulanabilmektedir. Kapasitif veya basınç tabanlı algılama teknolojilerine sahip olan dokunsal sensörlerden farklı olarak önerilen sistem muayene edilen yüzeyin şeklini alarak yüzeydeki kuvvet dağılımını ölçebilmekte ve böylelikle daha yüksek bir uzaysal çözünürlüğe ulaşabilmektedir. Önerilen sistemin performansının ölçülmesi için tümör benzeri sert silikon yumrular doku benzeri silindirik silikon örneklerin içine koyuldu. Daha sonra dokunsal sensörün bu tümör benzeri yumruları bulmadaki hassasiyetini ve keskinliğini ölçmek için sıkıştırma deneyleri yapıldı. 2 değişik boyutta, 2 değişik sertlikte ve 3 değişik derinlikte bulunan 11 tümör benzeri silikon yumru ile yapılan deneylerin sonuçlarına göre dokunsal sensör  $90.82 \pm 8.08\%$  hassasiyet ve  $89.80 \pm 12.66\%$  keskinlik gösterdi. Son olarak 12 insan deneğinin katılımıyla aynı silikon örnekler üzerinde elle muayene deneyleri yapıldı. Çıkan sonuçlar ile dokunsal sensör sonuçları karşılaştırıldı. Dokunsal sensörün silikon örnekler içindeki derin yumruları bulma performansının insanlarınkine göre daha yüksek olduğu, insanların ise silikon örneklerin yüzeyine yakın yumruları bulma performansının dokunsal sensörünkine göre daha yüksek olduğu tespit edildi.

## LIST OF SYMBOLS

$R^2$	Goodness of fit
$p$	Significance Level
$TP$	True positive
$FP$	False positive
$TN$	True negative
$FN$	False negative
$PPV$	Positive predictive value
$NPV$	Negative predictive value



## LIST OF ABBREVIATIONS

BSE	Breast Self-Examination
CBE	Clinical Breast Examination
FFDM	Full-Field Digital Mammography
MRI	Magnetic Resonance Imaging
UE	Ultrasound Elastography
MRE	Magnetic Resonance Elastography
TI	Tactile Imaging
PEF	Piezoelectric Finger
IR	Infrared
LED	Light-Emitting Diode
PCB	Printed-Circuit Board
TDM	Time-Division Multiplexing
ADC	Analog-to-Digital Converter
2AFC	Two-Alternative Forced Choice
SDT	Signal Detection Theory
PDF	Probability Density Function

## LIST OF FIGURES

Figure 1 a) Our tactile sensor. b) Cross-section of the tactile sensor.....	11
Figure 2 Data acquisition units of the proposed tactile imaging system.....	12
Figure 3 The calibration set-up of the tactile sensor.....	13
Figure 4 The calibration curve of a sensor element used in the tactile imaging system.....	14
Figure 5 The steps of the data processing: a) the tactile images of the comparison and the control groups (10 X 10) are spatially interpolated to 100 X 100, b) low-pass filtering is applied to the images to reduce the spectral noise, c) the tactile image of the comparison group is subtracted from that of the control group, d) the pixels at the edges are downgraded to eliminate the boundary effects.....	16
Figure 6 The cylindrical silicon samples with embedded inclusions used in the experiments. ...	18
Figure 7 The stress versus strain curve for the hard tumor-like inclusion (E = 78 kPa at 1% strain and E = 91 kPa at 5% strain), for the soft tumor-like inclusion (E = 56 kPa at 1% strain and E = 60 kPa at 5% strain), and for the tissue-like silicon medium (E = 11 kPa at 1% strain and E = 20 kPa at 5% strain) .....	18
Figure 8 The mechanical compression device used in our study to characterize the performance of our tactile sensor.....	19
Figure 9 a) The histogram of average forces recorded for an exemplar tactile image. b) The probability density function for the same tactile image.....	22
Figure 10 The exemplar plots of probability density functions for the control and the comparison groups. The areas which are highlighted in the plots show a) True positives ( <i>TP</i> ), b) True negatives ( <i>TN</i> ), c) False positives ( <i>FP</i> ), d) False negatives ( <i>FN</i> ).....	22

Figure 11 The stimuli used in the manual palpation experiments.....	23
Figure 12 The tactile images of the silicon samples used in our experiments for the compression depth of 15 mm.....	26
Figure 13 The tactile images of the silicon samples used in our experiments for the compression depth of 19 mm.....	27
Figure 14 The percentage of the false diagnoses made by the subjects. ....	29

## LIST OF TABLES

Table 1 The statistical measures of performance for the tactile sensor.....	28
Table 2 The statistical measures of performance for the human manual palpation. ....	30
Table 3 The comparison of the performances of the tactile sensor and the human manual palpation (statistically significant if Z-Score > 1.96 or Z-Score < -1.96).....	31

## Chapter 1

### 1. INTRODUCTION

#### 1.1 Breast Cancer

According to the statistics reported for 2008, breast cancer is the most common type of cancer among women, with an estimated 1.38 million new cases (23% of all the cancers) and the second most common cancer worldwide in both sexes (10.9% of all the cancers) [1]. The survival from breast cancer is critically dependent on early detection and treatment. For example, the 5-year survival rate for stage-0 breast cancer is 92%. On the other hand the 5-year survival rate for stage-4 breast cancer is 13% [2, 3]. To improve survival rate in this disease, patient must be identified at an early stage of breast cancer. However, in developing countries, majority of the population does not have access to the sophisticated medical devices and methods used for screening and diagnostic due to the high cost of these devices [4].

Breast cancer is a type of cancer originating from breast tissue; most commonly starts in the cells that line the milk ducts or the lobules that supply the ducts with milk. What causes breast cancer is still not known for certain; however there are some risk factors associated with gender, age, family history of breast cancer, and hormones. For example, being a woman is the major risk for breast cancer. It is more than 100 times more common in women than in men [5, 6]. Also, the risk factor increases with age. For example, breast cancer rates are 8-fold higher in women who are 50 years old, in comparison with women who are 30 years old [7]. If a woman has already had breast cancer in one breast, she has a greater chance of developing a new cancer in the other

breast. The risk of breast cancer is about two times higher among women who have a first-degree relative (mother, sister, or daughter) with this disease. About 5% to 10% of all breast cancers are hereditary. Breast cancer risk is increased in women with exposure to sex hormones, particularly estrogen [8].

If a tumor is limited to few cell layers and does not invade and destroy surrounding tissues or organs, it is considered benign (non-cancerous). In contrast, if the tumor spreads to surrounding tissues or organs, it is considered malignant (cancerous) [8, 9]. When breast cancer is discovered at an early stage and cancer cells have not grown into the surrounding tissue, this type of tumor is called as non-invasive, in situ tumor. On the other hand, if breast cancer penetrates the membranes that surround the lobules or ducts, it is known as infiltrating or invasive tumor [10]. The most common place of a tumor is the upper outer quadrant of the breast in both in situ and invasive tumors [11].

Treating breast cancer at its early stage of onset is crucial and highly dependent on the performance of the breast cancer imaging and diagnosis modality. Although various sensing methods and devices have been developed, only few of them have high sensitivity, acceptable specificity, good accuracy, ease of use, acceptability to population being screened (considering discomfort and time) and are low cost [12, 13]. In medical tests, sensitivity is defined as the percentage of sick people who are correctly diagnosed as having the condition and specificity is the proportion of healthy people who are correctly identified as not having the condition. Ideally, sensitivity and specificity aims to accomplish 100% success so that no one is mistakenly identified as healthy or sick. Currently, self-examination (BSE), clinical breast examination (CBE), mammography, ultrasonography, magnetic resonance imaging (MRI) are the most commonly used methods for screening and diagnostics of breast cancer.

## **1.2 Breast Cancer Imaging**

### **1.2.1 Conventional modalities**

#### **1.2.1.1 BSE**

Breast-Self Exam (BSE) is regular examination of breasts by women via palpation. It is a costless and non-invasive procedure for early detection of abnormalities. However, its effectiveness is highly dependent on the examiner's proficiency. Even if the examiner has good skills, it is often difficult for humans to detect small size tumors less than 1 cm in diameter [14]. Also, BSE does not allow one to differentiate between tumor types or provide quantitative and objective information about the tumors. In fact, it was argued that BSE does not provide any improvement in breast cancer mortality rates compared to those with no screening, but those screened patients even underwent biopsy twice as many times [15]. Nevertheless, BSE is still useful for detecting suspicious lesions [16, 17], but it is suggested that a woman who wants to perform regular BSE should be trained by a health professional and/or have her technique reviewed periodically [18].

#### **1.2.1.2 CBE**

CBE involves regular examination of breast by a health professional. Similar to BSE, CBE requires examiner's proficiency. An annual CBE is suggested for women older than 40 years of age [18]. Many physicians express a low confidence in their clinical breast examination skills [19, 20], which results in increased number of investigations, unnecessary biopsies, and false diagnosis [20, 21]. In addition, CBE and the associated reporting procedures are not standardized and consistent. On the other hand, it can detect the tumors missed by mammography, [22, 23] and it is also important for those who do not have access to more sophisticated devices and techniques at all. Furthermore, Brown et al. reported that the cost effectiveness of CBE

is 3.5 folds better than the cost effectiveness of mammography while CBE detects 34% fewer breast cancers [24]. The average size of tumors detected by CBE is 2.1 cm in diameter [25].

### 1.2.1.3 Mammography

Mammography is the most commonly used breast screening modality today. It is the process of compressing the breast tissue between two plastic plates and applying low-dose amplitude X-rays. Unlike BSE and CBE, mammography requires certain medical equipments such as a dedicated X-ray machine, radiographic film and developing chemicals, a trained technologist to use the machine and a radiologist to interpret the films. Especially, the compression causes considerable discomfort to patient. The mean radiation dose in mammography is approximately 4-5 mGy, but the applied dosage varies with the breast density [26]. As the dose increases, the risk of further breast cancers due to the radiation increases [27]. For this reason, mammography is not recommended for women under the age of 30 since the incidence rate of breast cancer for that group is low and their breast densities are high. Also, screening by mammography is not applicable for women who are pregnant or have breastfed within the last year. Also, mammography is unable to examine breast tissue near the chest wall and axilla. Armstrong et al. [26] argued that the risk for death due to breast cancer from the radiation exposure involved in mammography screening is small and is outweighed by a reduction in breast cancer mortality rates from early detection. In full-field digital mammography (FFDM), low energy x-rays pass through the breast in the same way as the conventional mammograms, nevertheless the images are recorded by means of an electronic digital detector instead of the film. Therefore, the output can be displayed on a digital environment or eventually printed on a film again. The advantage of the FFDM is that a health professional can electronically manipulate the resulting image by magnifying it, changing its contrast, or altering its brightness. Also, FFDM is more sensitive than the conventional mammography in young women under the age of 40 and in women older than 40 having dense breasts [28, 29].



However, the devices used for FFDM are 10 to 40 times more expensive than the conventional ones.

#### **1.2.1.4 MRI**

Magnetic resonance imaging (MRI) is a breast cancer screening modality that uses a powerful magnetic field to align the magnetization of the nuclei in the hydrogen atoms that makes the water content in the breast tissue with the oxygen atoms and pulses of radio wave energy to alter the alignment of this magnetization. This causes hydrogen nuclei to produce a rotating magnetic field detectable by the scanner so that the breast tissue and the tumors inside the breast tissue can be imaged [30]. MRI is good at imaging dense breasts of younger women, implants which are often a problem for mammography owing to possible leak in the implant or rupture due to the squeezing, and smaller lesions often missed by mammography. MRI also helps to determine the stage of breast cancer. Furthermore, MRI does not use radiation and can be applied to pregnant women though its effect on the fetus is still not known [31]. MRI breast cancer detection process requires the patient to lie down for half an hour to an hour and half without moving, which can be uncomfortable [32]. MRI is not only a long but also a costly technique. Moreover, the false positive findings are a problem in MRI and it is difficult to differentiate between benign and malignant tumors using MRI [33].

#### **1.2.1.5 Ultrasound**

Ultrasound refers to sound wave with a frequency above the audible range of human hearing, 20 kHz. There are several modes of ultrasound and most common ones are B-mode and Doppler mode. In medicine, ultrasonography is a screening technique used to image superficial structures such as muscles, brain or breast. B-mode ultrasonography uses emitted and reflected sound to create an image of the breast. Whenever a sound wave encounters an object with a different density, part of the sound wave is reflected back to the source and is detected as an echo. The time it takes for the

echo to travel back to the probe is measured and used to calculate the depth of the tissue interface causing the echo. B-mode ultrasonography is frequently used as a follow-up test for the assessment of mammographically or clinically detected breast masses to obtain supplemental information. Also, it is used to characterize lesions of women who cannot undergo mammography owing to pregnancy or young age [34]. However, ultrasonography requires well trained skilled operator. Since the purpose of the ultrasonography is the examination of a suspicious area in the breast, diagnosing the whole breast with ultrasonography is labor-intensive and operator-dependent [35]. Also, examination techniques are not standardized and the interpretation of the results shows variations. In Doppler Sonography, Doppler Effect is used to assess whether structures are moving towards or away from the probe. By calculating the frequency shift, its speed and direction can be determined and visualized. Cosgrove et al. [36] found that in contrast to 96% of benign lesions, 99% of malignant lesions contained blood vessels and showed colored Doppler signal.

#### **1.2.1.6 Elastography**

Elastography is another method that utilizes elastic modulus or strain images to detect or characterize tumors in the breast tissue. Since a tumor is typically stiffer than the surrounding normal tissue, it can be detected based on its measured elastic modulus. When breast tissue is stimulated via compression or low-frequency vibrations and the resulting deflections are measured by ultrasound, it is called ultrasound elastography (UE). On the other hand, if an electro-mechanical driver vibrates the tissue by generating acoustic shear waves and the propagation of the waves inside the tissue are imaged by MRI, it is called magnetic resonance elastography (MRE). McKnight et al. [37] reported that the mean shear stiffness of breast carcinoma is 418% higher than the mean value of surrounding breast tissues and stated that further research is needed to characterize suspicious breast lesions and improve MRE.

### 1.2.2 Tactile imaging

Tactile imaging (TI) is one of the emerging non-invasive medical imaging techniques that can be used to detect tumors inside the breast tissue. TI involves applying compression to the breast tissue with a probe having an array of pressure sensors at the tip to measure the pressure distribution at the contact area. TI can estimate the shape, size, and location of a tumor by comparing its stiffness with the surrounding healthy tissue. Young's modulus measurements of breast specimens showed that healthy tissue has a significantly lower elastic modulus than that of cancerous tissue [38-40]. Benign and cancerous tumors in the tissue have distinguishable material and geometric properties as reported in [41, 42]. TI is a relatively new method for breast examination; hence, the number of devices available for clinical use is limited. Medical Tactile Inc., (Los Angeles, CA, USA) produced a TI device under the trade name of SureTouch [43]. The system includes a probe, a processor unit and a computer. The probe consists of 192 (16x12) pressure sensors covering an area of 40 mm x 30 mm. The processor unit can make 20 measurements per second and transfer the measured data to a computer through USB interface [44]. Kaufman et al. [45] examined 110 patients with breast masses and estimated the geometrical and material properties of these masses from the recorded tactile images using SureTouch. Using the same TI system, Egorov et al. [44] conducted experiments with a silicon model and also clinical experiments. In their experiments, the examination was performed in two consecutive steps: (1) a general examination by linear sliding of the probe, and then (2) a local examination by making circular motions. If a suspicious area is detected in the first step, then a more detailed examination is performed in the second step. To process the collected data, several signal processing techniques have been used: low pass noise-cutting, two-dimensional noise-removal, background subtraction, signal thresholding, pixel neighborhood rating, sub-sampling, and two-dimensional interpolation. They used  $\text{Max/Base} > \text{noise criterion}$  (i.e. the max pressure recorded for an inclusion divided by the base pressure of the surrounding

tissue is greater than some predefined threshold value) and a neural network algorithm to detect the inclusions. They concluded that the performance of their TI system was better in detecting inclusions than that of manual palpation. Assurance Medical Corp. (Hopkinton, MA, USA) [46] developed a TI system consists of a hand-held probe with 146 (16x26) piezo-resistive pressure sensors, an electromagnetic position tracker embedded into the probe, and a computer and a DAQ to sample the signals. The pressure sensors have a range of 0-34 kPa. The computer acquires data from the tracker and the pressure sensor data at 200 Hz. The tracker records the relative position and rotation of the probe to help with the construction of the 3D tactile map of the breast. The voice commands guides the clinician to help her/him exert the desired average pressure to the breast tissue to reduce the variations between images [47]. Wellman et al. [48] proposed inverse models to estimate the size and the shape of a lump in breast tissue based on the pressure distribution recorded by this device. They stated that their forward and inverse algorithms provided accuracy at least twice as good as either CBE or ultrasound. Yegingil et al. [49] developed a piezoelectric finger (PEF) which consists of a driving piezoelectric actuator at the top, a sensing electrode at the bottom and a stainless steel layer in the middle. PEF could both apply force and sense the corresponding displacement. When electric field is applied to the driving piezoelectric actuator, the finger bends and the amount of deflection is measured by the sensing electrode. Elastic modulus, shear modulus, and Poisson's ratio of soft polymer samples were measured via indentation and consequently, elastic and shear moduli maps in 2D were constructed. The depth and elastic modulus of an inclusion in a polymer sample were determined by using two PEFs having in different sizes and an empirical model made of two springs. The smooth and rough surface inclusions were differentiated from each other based on the ratio of shear modulus ( $G$ ) to elastic modulus ( $E$ ). Omata et al. [50] developed a TI system consists of an array of 64 sensors for the examination of breast stiffness. Each sensor included driving and sensing PZT ceramic elements and a vibration rod with a spherical tip. The elasticity of an object is estimated based on the shift in the resonance frequency of the sensor when the rod is contacted the object.

### 1.2.3 Our approach: Opto-Electro-Mechanical Tactile Imaging

Even though, there are only a few TI systems available for breast cancer imaging and limited clinical data reported about their performance, it shows significant potential to address the needs in breast cancer detection and diagnostics. In this paper, we present a novel opto-electro-mechanical TI system, which can be utilized to guide the clinician or the self-user for non-invasive detection of lumps in breast tissue [51]. This system includes an array of tactile sensors, a processor unit and a computer to detect breast lesions. Compared to the conventional imaging techniques such as mammography, MRI and ultrasonography, the proposed system is cost effective and can be used at home. Furthermore, our system does not have any side effects compared to conventional imaging modalities during or after the examination and it can potentially be used by women who are pregnant or breastfeeding. Compared to the other TI systems utilizing capacitive or piezo-based sensing technologies, the proposed TI system conforms to the palpable object, which results in distributed force sensing and may lead to higher spatial resolution if small size sensors are used. Moreover, capacitive systems typically require complex circuitry and hence more prone to electrical noise and piezoelectric systems drive high voltages.

In order to demonstrate the practical use of the proposed TI system, 11 tissue-like cylindrical silicon samples containing tumor-like spherical silicon inclusions in 2 different sizes (large and small), and stiffnesses (hard and soft), located at 3 different depths (shallow, intermediate and deep), were prepared. Subsequently, compression experiments were performed with the TI system to detect embedded inclusions. In addition, manual palpation experiments were designed to measure the performance of 12 human subjects on the same silicon samples. Finally, the performance of the TI system in compression experiments was compared to that of the human subjects in manual palpation experiments to derive conclusions.

## Chapter 2

### 2. METHODS AND MATERIALS

#### 2.1 Design of the Tactile Sensor

Our TI system consists of 100 infrared (IR) emitter-detector sensors (QRD1313, Reflective Object Sensor; Fairchild Semiconductor) arranged in a 10×10 array shown in Figure 1 (a). The sensor elements are powered by an external, regulated power supply (5 V DC). The emitter of a QRD1313 reflective sensor is an IR light-emitting diode (LED), and the detector is a photo-darlington transistor for higher sensitivity, molded in a plastic case permitting through IR light rays. The sensor elements are soldered on a double-sided printed-circuit board (PCB) and housed in a prismatic aluminum casing with a square base, as illustrated in Figure 1 (b). The side length and the height of the TI system are 9.2 cm and 3.0 cm, respectively. The spatial resolution of the TI system is 2.8 mm.

The sensor elements are covered by a silicon-rubber membrane and optically isolated from each other by a spacer grid. Also, the outer surface of the rubber membrane was painted in black to block ambient light. The IR light rays emitted from the LEDs reflect off from the white colored inner surface of the membrane and reach to the detectors. This reflection is modulated by the force applied to the membrane's outer surface as a result of the interaction between the TI system and the palpated object, causing the membrane to deflect towards the detectors. The interaction force is transmitted from the palpated object to the membrane via contour pins, which conform to the shape of the object.

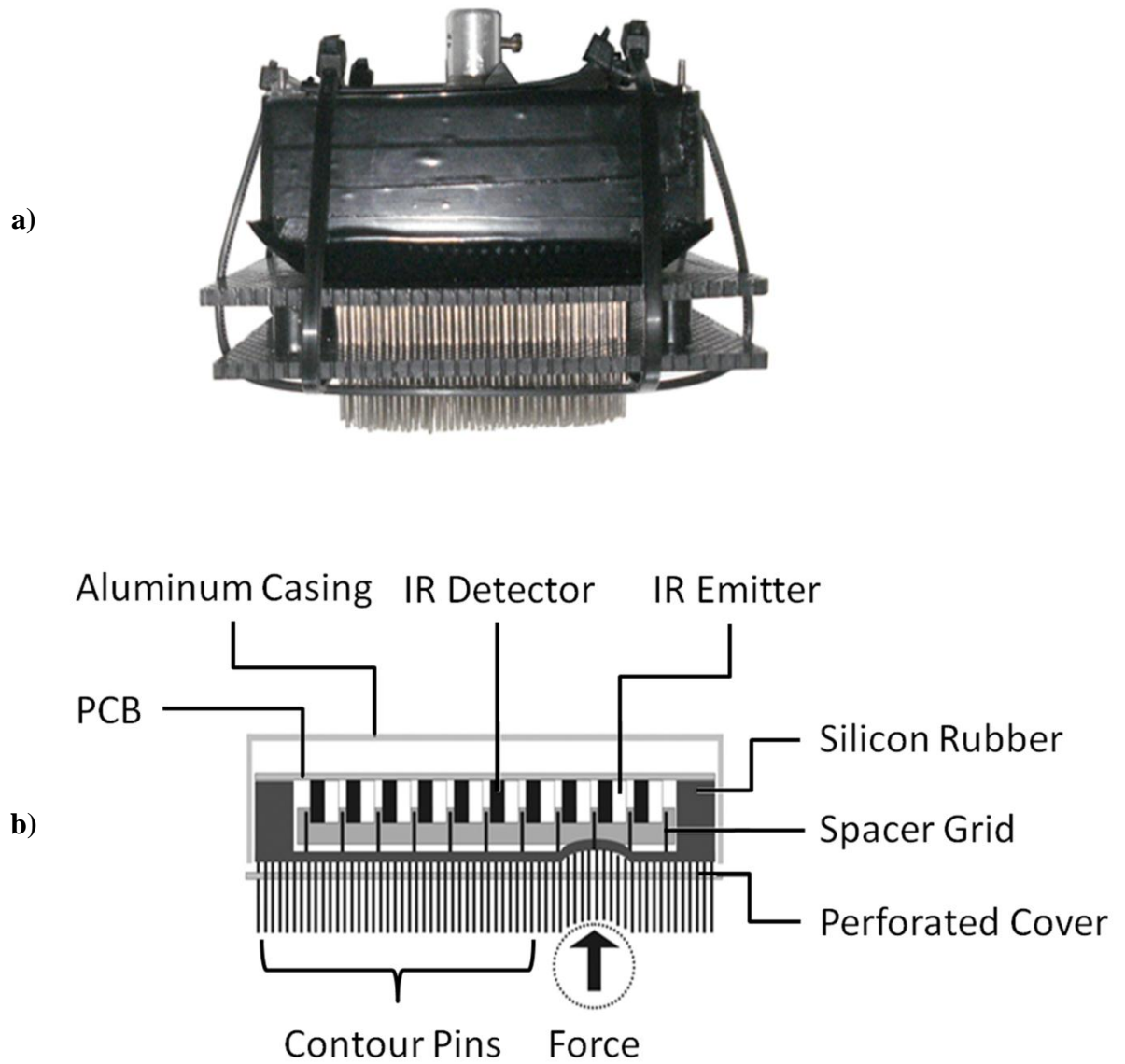


**Figure 1** a) Our tactile sensor. b) Cross-section of the tactile sensor.

## 2.2 Data Acquisition

The light intensities measured by the IR detectors are first transmitted to the processor unit via a flat cable and then to a 16-bits analog-to-digital converter (ADC) card (NI6034, National Instruments) via a single analog channel using the time-division multiplexing (TDM) method. In this method, 10 data points from each sensor element are acquired at each multiplexing cycle. Since the sampling rate of the ADC card is 100 kHz, one multiplexing cycle (the output from the entire array) takes 0.01 s ( $0.01 \text{ ms} \times 100 \text{ sensors} \times 10 \text{ data points}$ ) and hence the actual scan rate of the system is 100 Hz. The flow of the measured signal from the sensors to the ADC card connected to a PC is shown in Figure 2. The processor unit amplifies the multiplexed data and applies offset shifting to the signal to match the input sampling range of the ADC card. The ADC card decodes the incoming analog signal with the help of a synchronization pulse generated by the processor unit at each multiplexing cycle. The light-intensities measured by the IR detectors and then acquired through the ADC card are converted to force values via a calibration process.

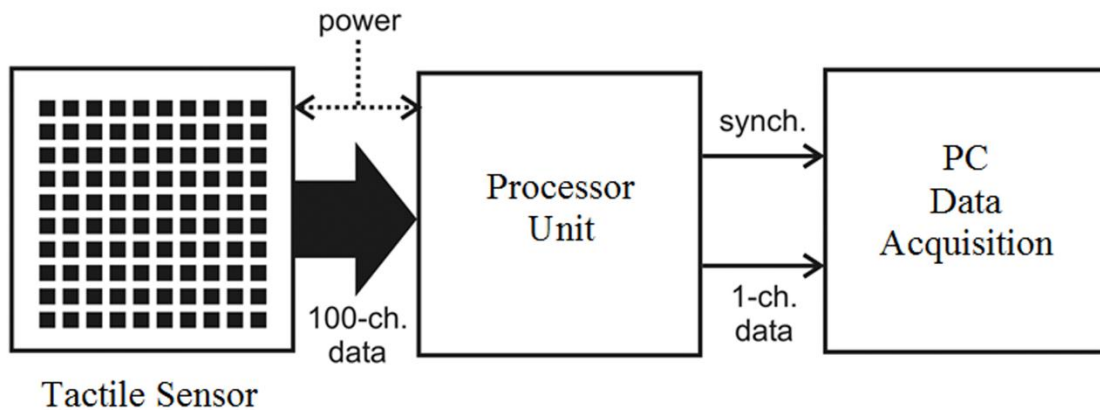


**Figure 2** Data acquisition units of the proposed tactile imaging system.



### 2.3 Calibration

For calibration, first, an indentation probe attached to an XYZ micromanipulator (KITE-R, World Precision Instruments, Inc.) as shown in Figure 3 was slowly pressed to each grid point on the outer surface of the silicon rubber membrane facing a sensor and then, the light intensity values measured by the IR detectors and the force response measured by a digital balance (440-49N, KERN) were recorded. As a result, the calibration curve of each sensor element in the range of 0-5 N was obtained. Subsequently, linear regression analysis was performed to obtain the best-fit equations and the goodness of fit ( $R^2$ ) values. The calibration curve of an exemplar sensor element is shown in Figure 4.

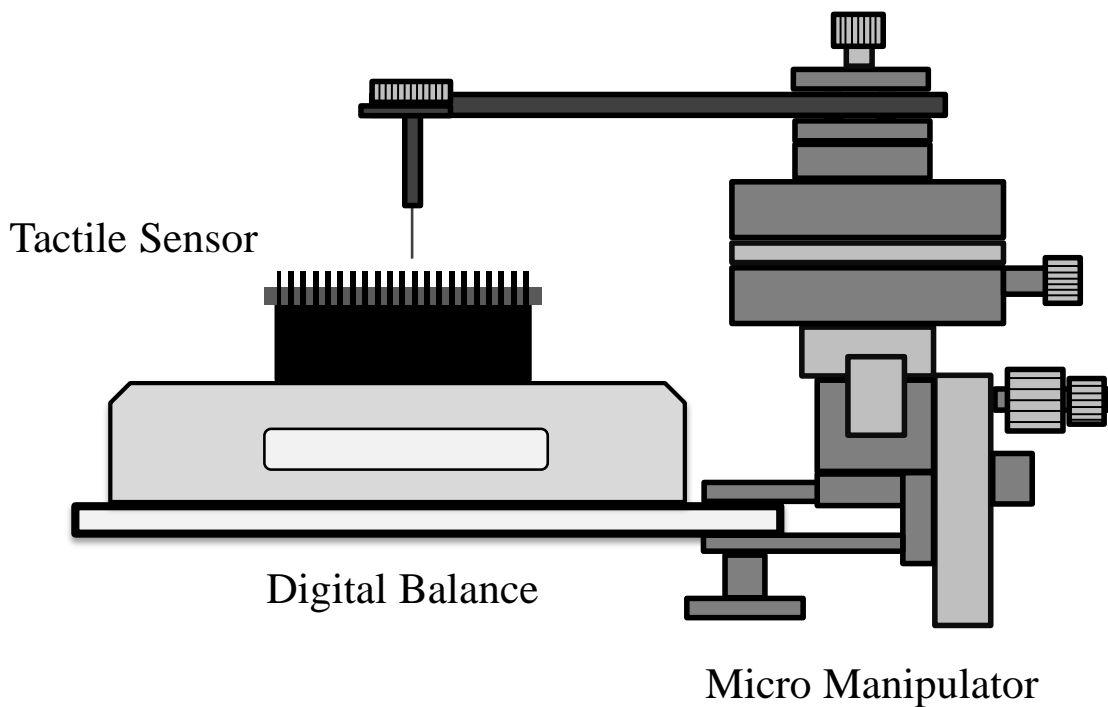


**Figure 3** The calibration set-up of the tactile sensor.

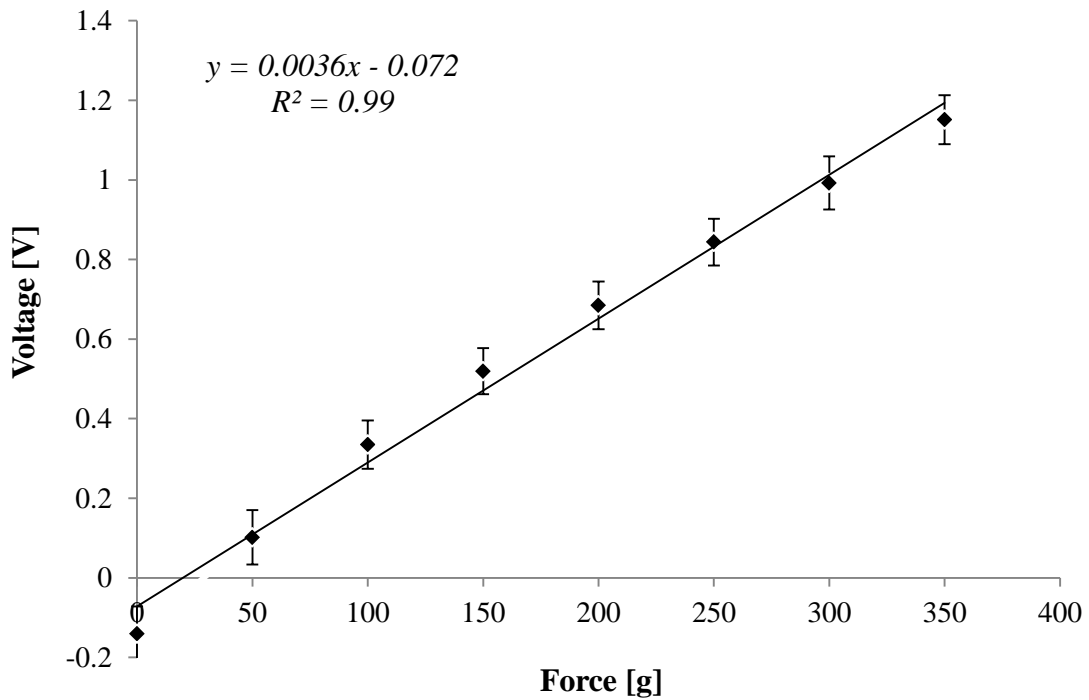


**Figure 4** The calibration curve of a sensor element used in the tactile imaging system.

The average force sensitivity and the average zero error of the tactile sensor was measured as 0.003746 V/g and 0.094 V, respectively. This offset (0.094 V) was compensated later during the data processing. Furthermore, the average value of  $R^2$  for 100 sensors, which shows the goodness of the fit, was calculated as 0.9128. Note that approximately 10% of the sensors located at the edges did not show a linear behavior ( $R^2 < 0.9$ ) due to the boundary effects.

## 2.4 Data Processing

The data processing involves four major steps: spatial interpolation, low-pass filtering, background subtraction and thresholding (see Figure 5).

- 
- a) **Spatial Interpolation:** The sensor data is acquired in units of force from the  $10 \times 10$  sensor array. It is spatially interpolated along the x and y axes to give an output force array of 100 by 100 elements.
  - b) **Low-pass Filtering:** A digital FIR filter is designed with Kaiser Window, which can achieve a stop band attenuation of 65 dB. The spatial cutoff frequency is selected as 5 cycles per linear length of the tactile membrane (i.e. 0.82 cycles/cm).
  - c) **Background Subtraction:** The statistical difference between the force responses of the samples in the comparison group and the control sample is tested by Bonferroni-corrected two-sample t-test. The force values of a comparison sample which are significantly different than those of the control sample are selected to construct its tactile image.
  - d) **Thresholding:** Since the boundary sensors are more prone to artifacts and distortions, additional filtering is performed on the boundary pixels. After the background subtraction, the pixel in each tactile image having the maximum force value is determined by excluding the pixels at the boundaries first. Then, the area around that pixel is determined by an edge detection algorithm. This area is defined as the suspicious area and the force values of the pixels that are outside this area are set to zero.

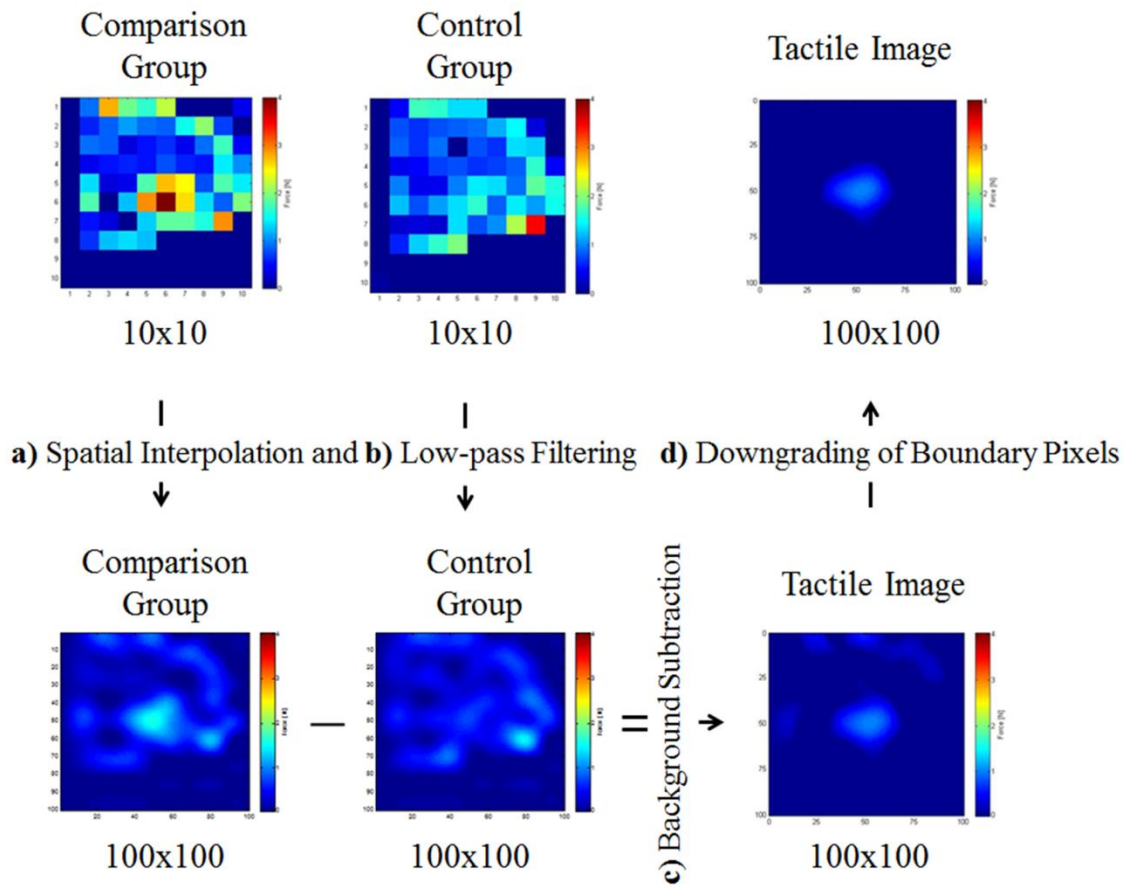


**Figure 5** The steps of the data processing: a) the tactile images of the comparison and the control groups (10 X 10) are spatially interpolated to 100 X 100, b) low-pass filtering is applied to the images to reduce the spectral noise, c) the tactile image of the comparison group is subtracted from that of the control group, d) the pixels at the edges are downgraded to eliminate the boundary effects.

## Chapter 3

### 3. EXPERIMENTS

Compression experiments were performed on tissue-like cylindrical silicon samples containing spherical silicon inclusions. The radius and the height of the cylindrical samples were 25 mm and 40 mm, respectively. The spherical inclusions in two different sizes (small/large) and in two different stiffnesses (soft/hard) were embedded into the cylindrical samples at three different depths (shallow/intermediate/deep) during the molding process (see Figure 6). The cylindrical sample containing a large and hard inclusion at zero depth was not used in the experiments since it was too easy to detect. The other eleven samples containing the inclusions of all other possible combinations ( $2 \times 3 \times 2 - 1 = 11$ ) were tested against the control sample having no inclusion in the compression experiments.

Commercial-grade silicon (Ecoflex Supersoft 0010, Smooth-On Inc.) was used to construct tissue-like cylindrical samples having a Young's modulus of 11 kPa and 20 kPa at 1% and 5% strains, respectively. The tumor-like spherical silicon inclusions were prepared in two different stiffness levels using Smooth-Sil 910 (Smooth-On Inc.) commercial silicon. The Young's modulus of the soft and the hard silicon inclusions were measured as 56 kPa and 78 kPa at 1% strain and 60 kPa and 91 kPa at 5% strain, respectively. The stress versus strain curves of the samples and the inclusions are shown in Figure 7. The inclusions were embedded into the silicon samples at  $h = 0$  mm (shallow), 10 mm (intermediate) and 20 mm (deep) depths. The diameters of the inclusions were  $d = 10$  mm (small) and 20 mm (large).

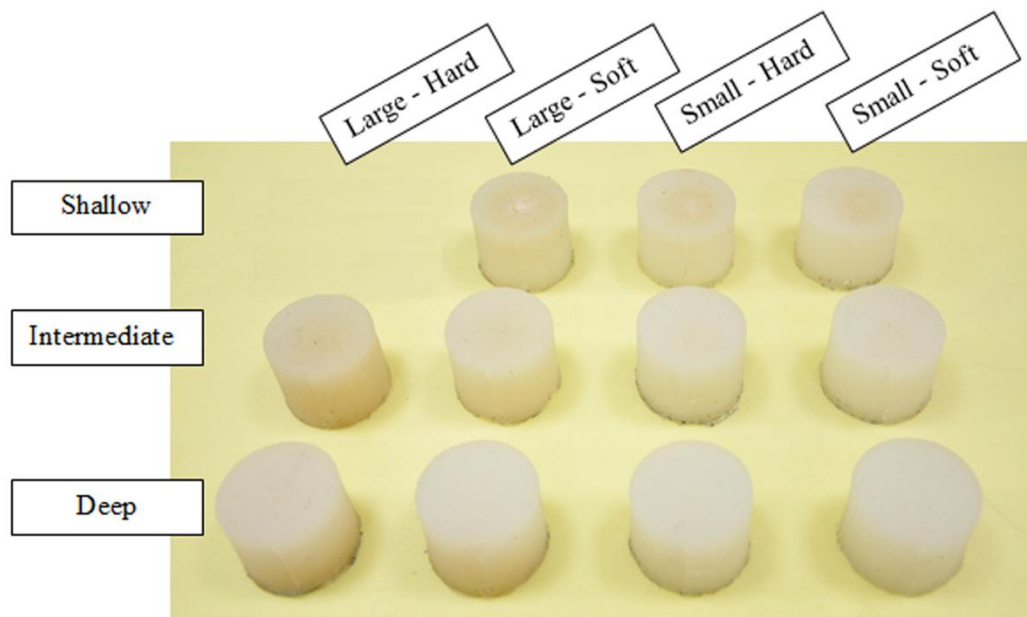


**Figure 6** The cylindrical silicon samples with embedded inclusions used in the experiments.

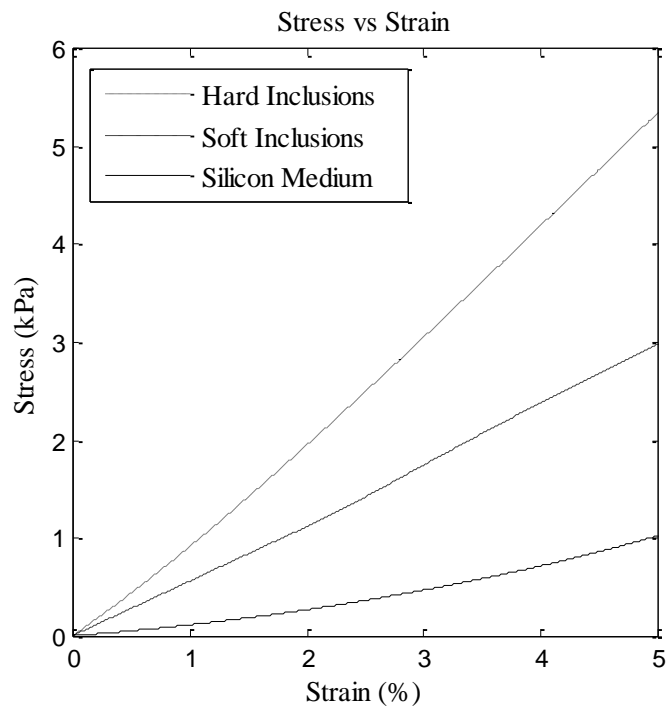


**Figure 7** The stress versus strain curve for the hard tumor-like inclusion ( $E = 78$  kPa at 1% strain and  $E = 91$  kPa at 5% strain), for the soft tumor-like inclusion ( $E = 56$  kPa at 1% strain and  $E = 60$  kPa at 5% strain), and for the tissue-like silicon medium ( $E = 11$  kPa at 1% strain and  $E = 20$  kPa at 5% strain)

### 3.1 Compression Experiments

The set-up developed in our laboratory [52] was used to conduct controlled compression experiments. The tactile sensor was attached to the moving shuttle of the power screw in our set-up as shown in Figure 8 and then commanded by a step motor to compress the cylindrical silicon samples slowly at a rate of 0.5 mm/s.

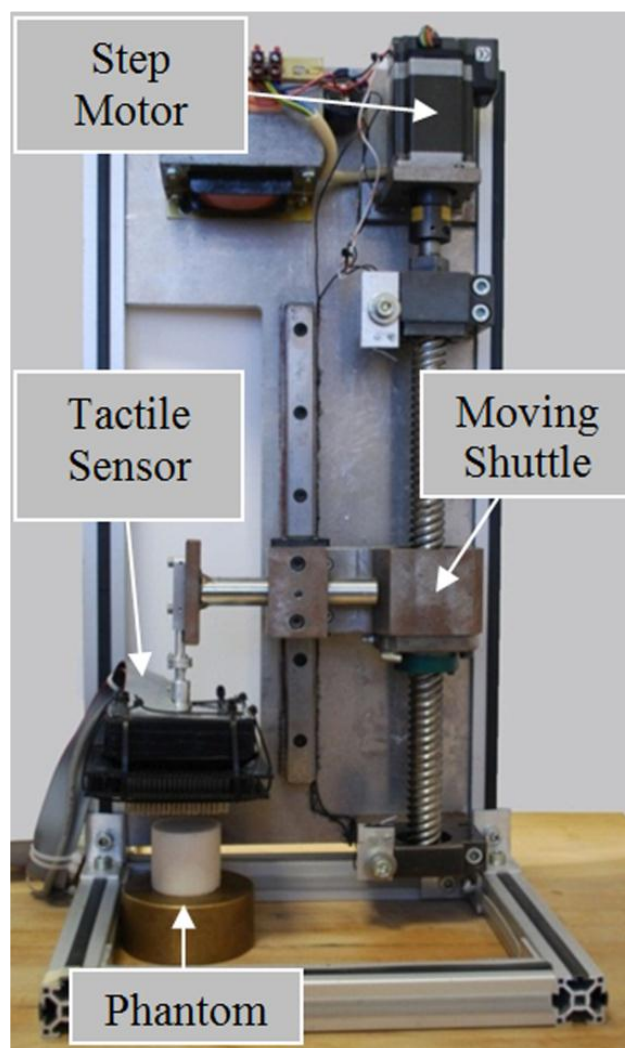


**Figure 8** The mechanical compression device used in our study to characterize the performance of our tactile sensor.

The cylindrical silicone phantoms containing an inclusion were compressed to the depths of 15, and 19 mm. These depths were selected based on the results of our earlier study, investigating the optimum compression depth [51]. For each depth, the compression experiment was repeated 20 times on each silicon sample containing an inclusion. Hence, the total number of compression experiments performed on the samples in the comparison group was 440 (2 depths X 11 samples X 20 repetitions). In addition, 20 compression experiments were performed on the control sample for each depth. Hence, the total number of compression experiments performed on the control sample was 40 (2 depths X 1 sample X 20 repetitions). Following the experiments, the collected data was processed using the steps discussed in Section 2.4.

### 3.2 Performance Evaluation of our TI system

Signal Detection Theory (SDT) was used to evaluate the performance of the TI system. For each sample with and without an inclusion, the average force output from each sensor was recorded for the compression depths of 15 mm and 19 mm. A histogram of the average forces measured by each tactile sensor was constructed for each sample and compression depth. To construct the probability distribution function (*pdf*), the number of occurrence for each bin was divided by the histogram area as shown in Figure 9 so that the total area of each *pdf* was equal to 1.

The bin width was critical in constructing the histograms: a small width would lead to the inclusion of unnecessary details into the histogram while a large width would result in a coarse histogram with no details. To find the optimum bin width for each histogram, the entropy of the bin heights was maximized as suggested in [53]. To determine if a silicon sample contained an inclusion, its *pdf* was compared to that of the silicon sample without any inclusion (i.e. control sample). Two-sample t-test with a significance level of  $p = 0.05$  was used to test the null hypothesis. If the null hypothesis



was true and the statistical analysis supported accepting the null hypothesis ( $TN$ ) or if the alternative hypothesis was true and the statistical analysis supported rejecting the null hypothesis ( $TP$ ), then the decision was considered as “right”. If the null hypothesis was true, but the analysis supported rejecting the null hypothesis ( $FP$ ) or if the alternative hypothesis was true, but the analysis supported accepting the null hypothesis ( $FN$ ), the decision was considered as “wrong”. In Figure 10, probability density functions of the control and the comparison groups are shown. The vertical line (i.e. criterion line) passing through the intersection of the curves divides the graph into four areas, labeled as “ $TP$ ”, “ $FN$ ”, “ $FP$ ” and “ $FN$ ”; which are used to calculate sensitivity, specificity, positive predicted value ( $PPV$ ), and negative predicted value ( $NPV$ ).

The sensitivity and the specificity are already defined in the Introduction section.  $PPV$  shows the proportion of the diagnoses with positive results, which are correctly detected. On the other hand,  $NPV$  indicates the proportion of the negative results, which are correctly detected. The formulation of the sensitivity, specificity,  $PPV$  and  $NPV$  are given as the followings:

$$Sensitivity = \frac{\sum TP}{\sum TP + \sum FN} \quad (3.1)$$

$$Specificity = \frac{\sum TN}{\sum TN + \sum FP} \quad (3.2)$$

$$PPV = \frac{\sum TP}{\sum TP + \sum FP} \quad (3.3)$$

$$NPV = \frac{\sum TN}{\sum TN + \sum FN} \quad (3.4)$$

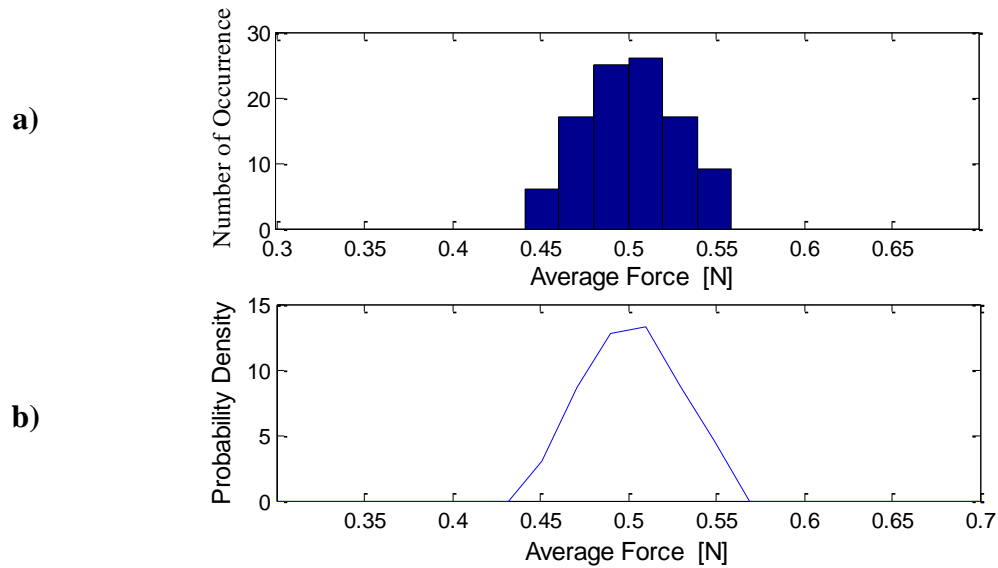


**Figure 9** a) The histogram of average forces recorded for an exemplar tactile image. b) The probability density function for the same tactile image.

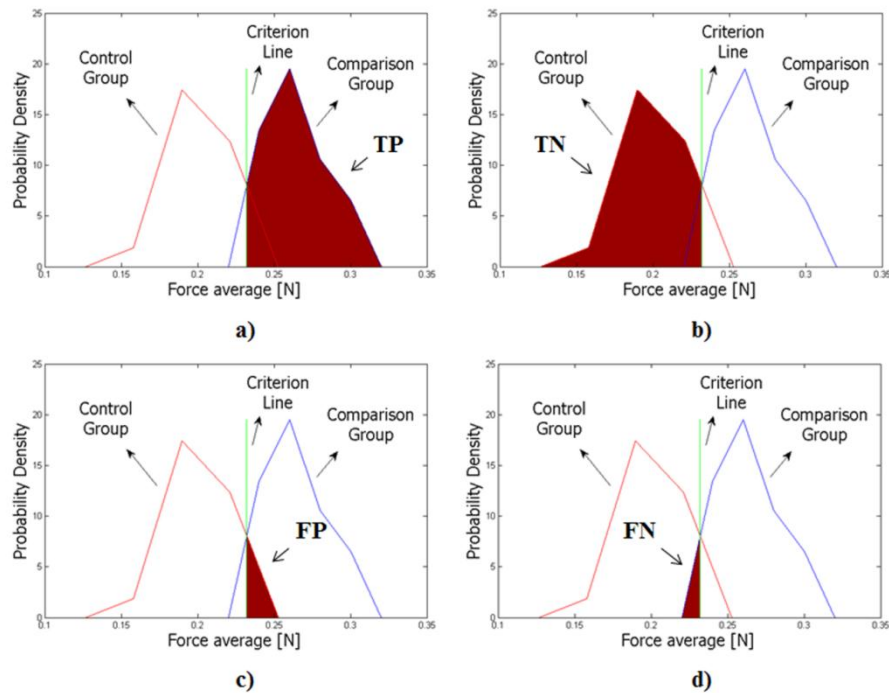


**Figure 10** The exemplar plots of probability density functions for the control and the comparison groups. The areas which are highlighted in the plots show a) True positives (*TP*), b) True negatives (*TN*), c) False positives (*FP*), d) False negatives (*FN*)

### 3.3 Manual Palpation Experiments

Manual palpation experiments were performed on the same silicon samples to detect tumor-like inclusions. 12 naive subjects (6 female and 6 male) were participated to the experiments (Age =  $25 \pm 1.5$ ). The experiment was designed with two-alternative forced choice (2AFC) method. The subjects were asked to use the finger pads of their middle three fingers to palpate a pair of silicon samples one by one to detect the silicon sample with an inclusion in 15 seconds (Figure 11). The samples were placed side by side and one of them always contained an inclusion, but its size, location, and the stiffness varied.

The subjects were asked to report their decisions to the experimenter as “LEFT” or “RIGHT” depending on which sample contained an inclusion. There were a total of 110 trials in the experiment (11 silicon pairs x 10 repetitions). The order and the relative location of the control sample in each trial (Left/Right) were randomized. Also, the subjects were blind-folded during the experiment to prevent any perceptual bias.



**Figure 11** The stimuli used in the manual palpation experiments.

### **3.4 Performance Evaluation for the Manual Palpation Experiments**

Each answer of the subjects in manual palpation experiments results in two outcomes in statistical means; detecting the correct sample with an inclusion, true positive (*TP*) and rejecting the other sample without an inclusion, true negative (*TN*) or incorrectly choosing the sample without an inclusion, false positive (*FP*) and incorrectly rejecting the sample with an inclusion, false negative (*FN*). For performance evaluation, the responses of the subjects were labeled accordingly first and then the sensitivity, the specificity, the positive predicted value (*PPV*), and the negative predicted value (*NPV*) were estimated from those labels.

## **Chapter 4**

### **4. RESULTS**

#### **4.1 TI System**

Tactile images for different inclusion depths, sizes, and stiffnesses at the compression depths of 15 and 19 mm are shown in Figure 12 and Figure 13. The results of the statistical analysis show that our TI system successfully detected all the embedded inclusions. Moreover, it detected the large and hard inclusions better than the small and soft ones. Table 1 tabulates the average measures of performance for the TI system. The results also show that the performance of our device was better in detecting shallow and deep inclusions than intermediate ones. It detected the deep inclusions better than the intermediate ones because deep inclusions were constrained by the lower boundary (bottom surface) of the silicon sample when the sample was compressed by the device. As a result, the forces transmitted by the inclusion to the contact interface were amplified.

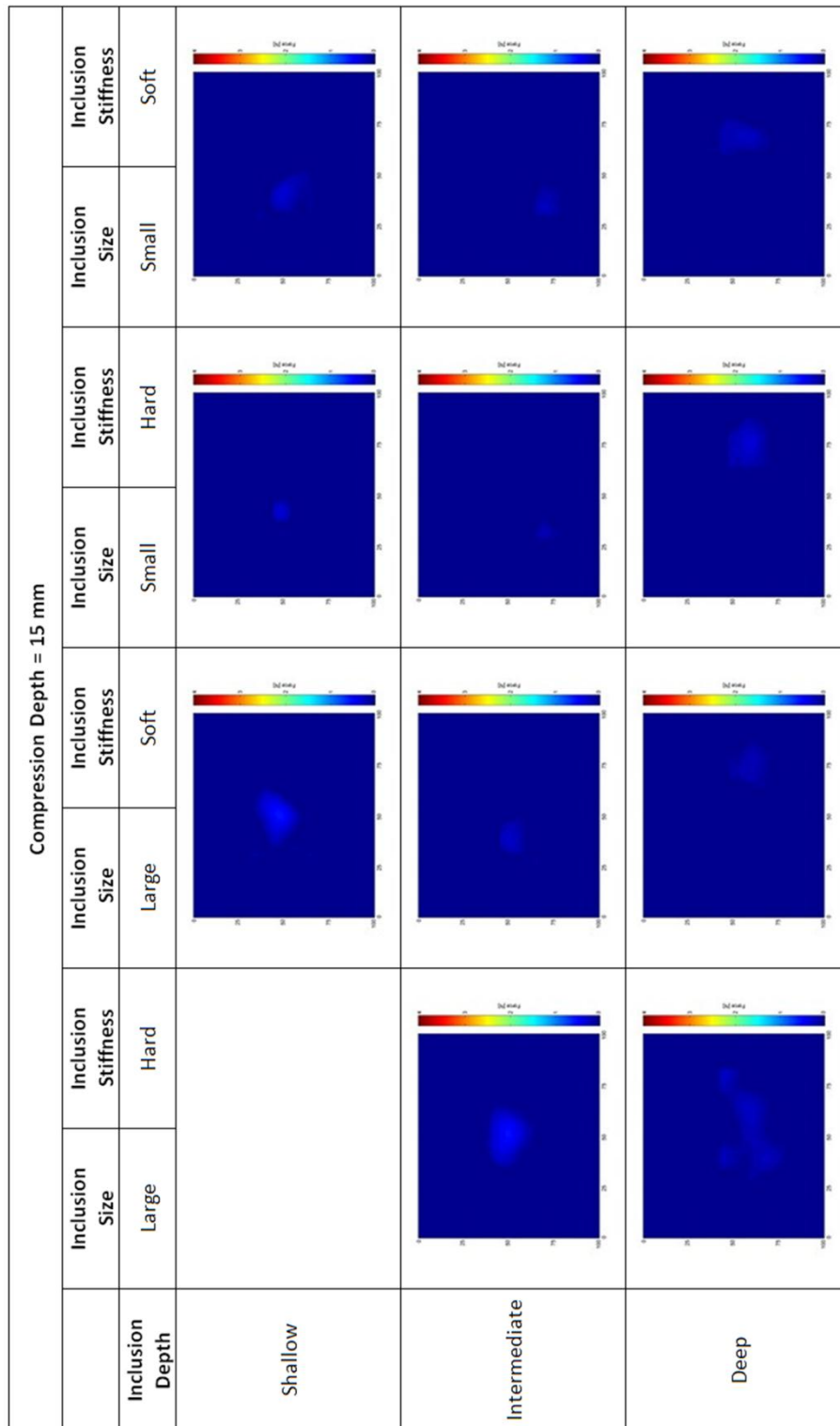


Figure 12 The tactile images of the silicon samples used in our experiments for the compression depth of 15 mm.

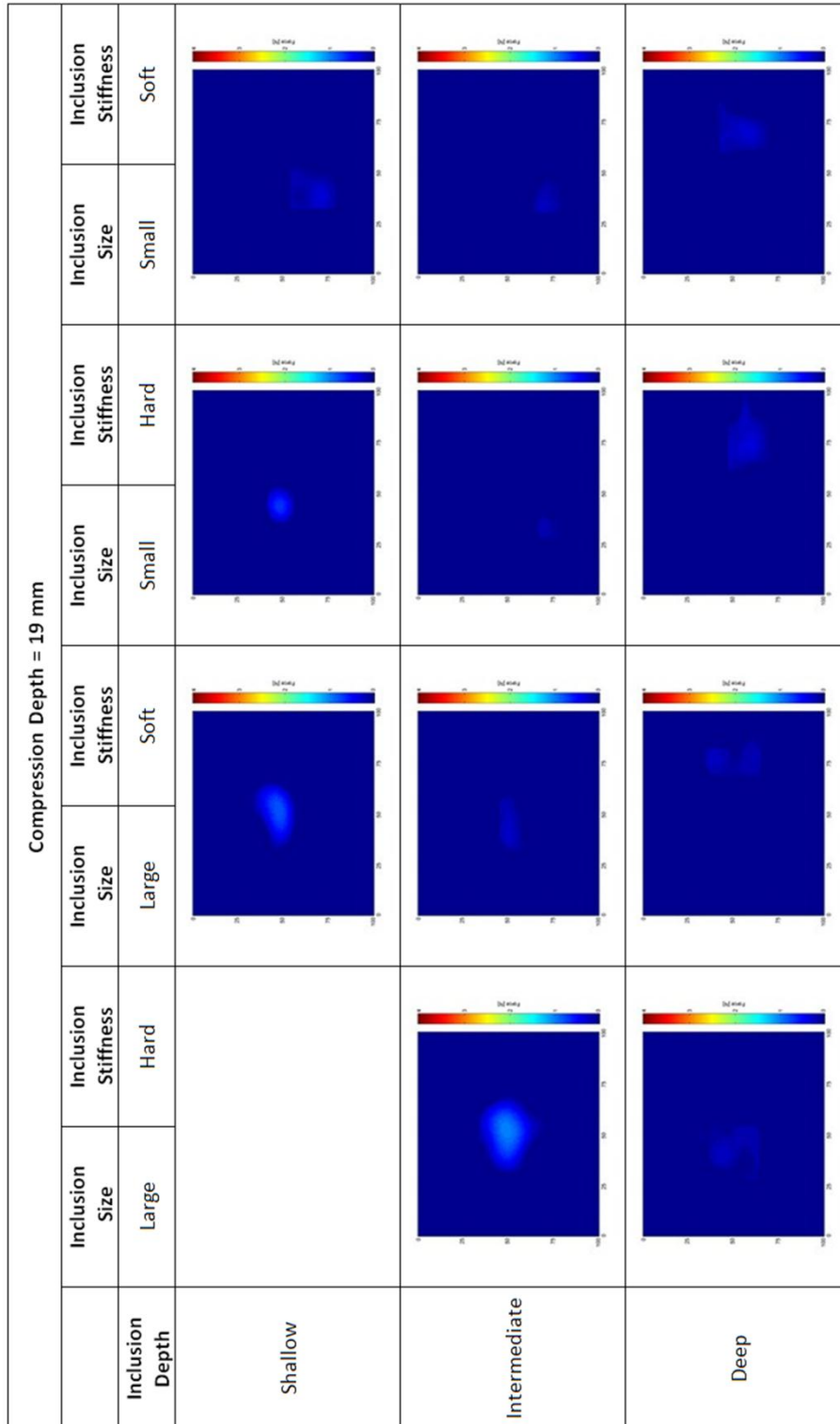


Figure 13 The tactile images of the silicon samples used in our experiments for the compression depth of 19 mm.

**Table 1** The statistical measures of performance for the tactile sensor.

Inclusion Depth	Inclusion Size	Inclusion Stiffness	Sensitivity	Specificity	PPV	NPV
Shallow	Large	Soft	96.72 ± 0.48%	98.75 ± 0.05%	98.73 ± 0.05%	96.78 ± 0.45%
		Hard	94.21 ± 2.02%	94.62 ± 5.61%	94.70 ± 5.44%	94.20 ± 2.21%
	Small	Soft	89.97 ± 0.08%	91.52 ± 3.89%	91.46 ± 3.61%	90.12 ± 0.31%
Intermediate	Large	Hard	96.29 ± 4.44%	95.88 ± 5.56%	95.93 ± 5.49%	96.25 ± 4.50%
		Soft	89.66 ± 1.81%	92.11 ± 3.90%	91.95 ± 3.83%	89.89 ± 1.97%
	Small	Hard	78.69 ± 5.85%	63.21 ± 8.37%	68.97 ± 7.63%	74.03 ± 6.77%
		Soft	72.56 ± 2.62%	66.08 ± 1.24%	68.13 ± 1.58%	70.68 ± 2.37%
		Hard	98.05 ± 0.61%	98.74 ± 0.99%	98.74 ± 0.98%	98.07 ± 0.58%
Deep	Large	Soft	92.83 ± 0.38%	94.67 ± 2.86%	94.62 ± 2.74%	92.97 ± 0.15%
		Hard	96.04 ± 1.13%	96.58 ± 3.86%	96.62 ± 3.79%	96.04 ± 1.23%
	Small	Hard	96.04 ± 1.13%	96.58 ± 3.86%	96.62 ± 3.79%	96.04 ± 1.23%
		Soft	94.04 ± 0.30%	95.62 ± 4.60%	95.62 ± 3.96%	94.12 ± 0.51%

## 4.2 Manual Palpation Experiments

The percentage of the false diagnoses made by the subjects with respect to the inclusion size, depth, and stiffness is shown in Figure 14. The results show that the false diagnoses made by the subjects increased as the inclusions were placed deeper. Also, it was easier for the subjects to detect the large and stiff inclusions than the small and soft ones. More interestingly, the percentage of the false diagnoses for the hard-small inclusions was less than that of the soft-large inclusions at the deepest level. In other words, the stiffness was more distinguishable than the size in detecting inclusions by manual palpation.

Table 2 tabulates the average measures of performance for the human subjects in detecting inclusions by manual palpation. Since 2AFC method was used for the design of the manual palpation experiments, the response of a subject in each trial automatically resulted in either success, (*TP* and *TN*) or failure (*FP* and *FN*). Consequently, the sensitivity values were equal to the specificity values and the *PPVs*



were equal to the *NPVs*. As observed from Table 2, all the statistical measures decreased as the depth of the inclusion was increased. In addition, the statistical measures were higher for the silicon samples containing large and hard inclusions.

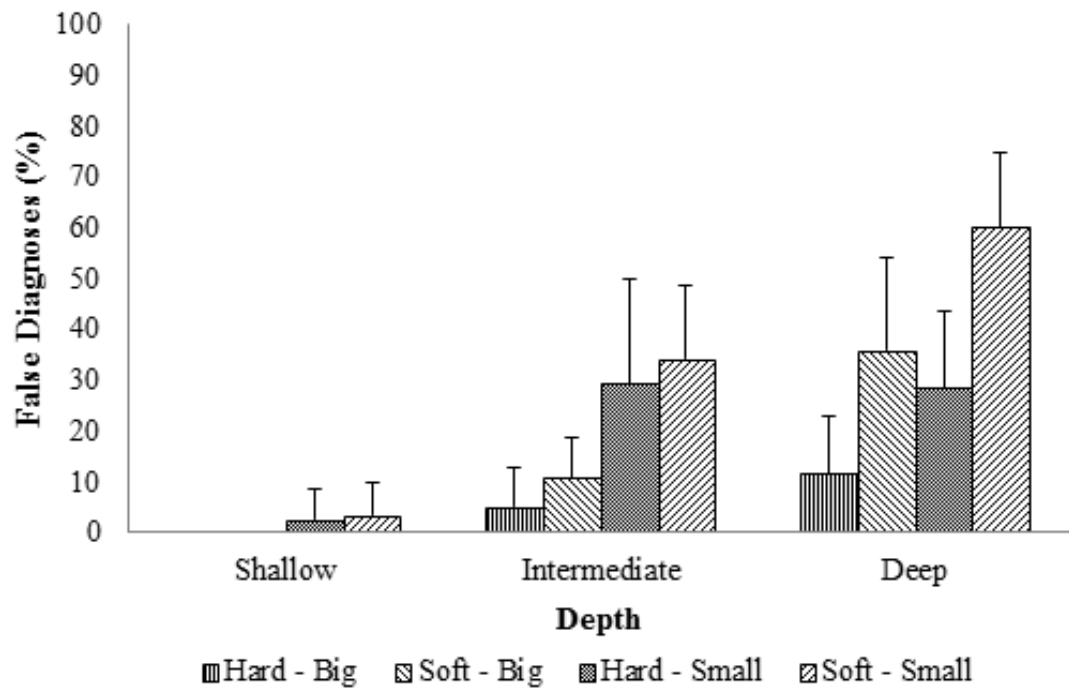


**Figure 14** The percentage of the false diagnoses made by the subjects.

**Table 2** The statistical measures of performance for the human manual palpation.

Inclusion Depth	Inclusion Size	Inclusion Stiffness	Sensitivity	Specificity	PPV	NPV
Shallow	Large	Soft	100.00 ± 0.00%	100.00 ± 0.00%	100.00 ± 0.00 %	100.00 ± 0.00 %
		Hard	97.22 ± 7.40%	97.22 ± 7.40%	97.57 ± 4.41%	97.57 ± 4.41%
	Small	Soft	96.53 ± 6.36%	96.53 ± 6.36%	96.53 ± 5.22%	96.53 ± 5.22%
Intermediate	Large	Hard	95.49 ± 7.42%	95.49 ± 7.42%	94.46 ± 7.61%	94.46 ± 7.61%
		Soft	87.85 ± 9.31%	87.85 ± 9.31%	89.50 ± 7.13%	89.50 ± 7.13%
	Small	Hard	67.71 ± 26.09%	67.71 ± 26.09%	62.60 ± 21.11%	62.60 ± 21.11%
		Soft	65.28 ± 14.14%	65.28 ± 14.14%	64.87 ± 15.24%	64.87 ± 15.24%
Deep	Large	Hard	89.24 ± 10.87%	89.24 ± 10.87%	87.83 ± 11.02%	87.83 ± 11.02%
		Soft	65.97 ± 17.66%	65.97 ± 17.66%	65.54 ± 21.44%	65.54 ± 21.44%
	Small	Hard	70.24 ± 16.73%	70.24 ± 16.73%	67.98 ± 15.95%	67.98 ± 15.95%
		Soft	39.06 ± 16.24%	39.06 ± 16.24%	42.93 ± 12.02%	42.93 ± 12.02%

### 4.3 Comparison of the TI system and the Manual Palpation

We conducted two-sample proportional z-test to compare the performance of the subjects in manual palpation experiments to that of the TI system in compression experiments (see Table 3). It was observed that the performance of the TI system was significantly better than that of the subjects in manual palpation experiments for the deep inclusions while the subjects performed better in detecting shallow inclusions except for the small-hard inclusion. There was no significant difference between the groups in the detection of the inclusions at intermediate depth.

**Table 3** The comparison of the performances of the tactile sensor and the human manual palpation (statistically significant if Z-Score > 1.96 or Z-Score < -1.96).

Inclusion Depth	Inclusion Size	Inclusion Stiffness	Sensitivity	Specificity	PPV	NPV
			Z-Score	Z-Score	Z-Score	Z-Score
Shallow	Large	Soft	<-1.96	-1.23	-1.24	<-1.96
		Hard	-1.11	-0.98	-1.12	-1.28
	Small	Soft	<-1.96	-1.59	-1.61	-1.94
		Hard	0.30	0.14	0.50	0.62
Intermediate	Large	Soft	0.42	1.04	0.62	0.09
		Hard	1.82	-0.70	0.99	1.81
	Small	Soft	1.16	0.12	0.51	0.92
		Hard	>1.96	>1.96	>1.96	>1.96
Deep	Large	Soft	>1.96	>1.96	>1.96	>1.96
		Hard	>1.96	>1.96	>1.96	>1.96
	Small	Hard	>1.96	>1.96	>1.96	>1.96
		Soft	>1.96	>1.96	>1.96	>1.96

## Chapter 5

### 5. DISCUSSION

#### 5.1 Discussion of our Work

##### 5.1.1 TI system

In this study, we developed an opto-electro-mechanical TI system to detect lumps in breast tissue. The TI system is designed to measure the stiffness contrast between the normal and abnormal breast tissue to detect suspicious lesions. In the design, an array of optical sensor elements consisting of an embedded IR emitting diode and a photodarlington transistor were used. These solid state optical sensors are compact, low cost, and widely available in the market. They took less space than individual emitter and detector sensors, which enabled us to use more sensors for the same contact area in our design. Also, the contour pins used at the contact interface reduced the cross-talk between the neighboring sensors. Nevertheless, the use of contour pins initially limited the spatial resolution of the TI system to 2.8 mm, which is the distance between two adjacent contour pins in our current design. On the other hand, the spatial interpolation applied to the tactile images during data processing improved this limit by almost 10-folds.

In our design, the silicon rubber membrane was fixed at the edges of the casing. While, this design allowed larger deflections at the center area of the TI system, it also limited the movement of the membrane at the edges and hence, resulted in greater variation in the sensor readings. Thereby, 10% of the sensor elements located at the edges did not show a linear behavior ( $R^2 < 0.9$ ) due to the boundary effects and hence

the raw values acquired from those sensors were downgraded during the post processing. In spite of this, the average value of goodness of fit was calculated as  $R^2 = 0.9128$ , which indicates the overall linearity of the sensor design.

### **5.1.2 Silicon samples**

The performance of the TI system was investigated through compression experiments performed on cylindrical silicon samples containing silicon inclusions. The results were compared to that of the manual palpation. In our experiments, the cylindrical silicon samples contained tumor-like silicon inclusions having a diameter of 10 and 20 mm, corresponding to stage 0 and stage 1 breast cancer, respectively [3]. The elastic modulus of the embedded inclusions was 5-7 times stiffer than that of the silicon samples at 1% strain. In experiments performed on ex-vivo breast tissue samples having fibrocystic disease and malignant tumors, a 3–6-folds increase in stiffness was observed while high-grade invasive ductal carcinoma causes up to 13-folds increase in stiffness compared to healthy tissue [40]. Hence, the size and the geometry of the inclusions used in our experiments as well as the ratio of stiffness of the silicon samples to that of the inclusions mimicked the breast tissue having a tumor.

### **5.1.3 Comparison of the TI system and the Manual Palpation**

The performance of the proposed TI system was compared to that of human manual palpation. It was seen that, the performance of the TI system was significantly better than that of the human subjects in manual palpation experiments for deep inclusions while human subjects performed slightly better in detecting shallow inclusions close to the contact surface. In detecting the inclusions at the intermediate depth, there was no significant difference between the sensor and the subjects. We speculate that the receptors lying in the subcutaneous tissue of the finger pad essentially sense the curvature of the shallow inclusions better than the TI system. However, as the inclusions are placed deeper in the samples, kinesthetic sensing of reaction forces rather

than tactile sensing of curvature and pressure changes becomes more dominant in detecting inclusions and the TI system becomes more effective.

## 5.2 Discussion with the Other Works

### 5.2.1 Comparison with the conventional breast cancer imaging modalities

The performance evaluation of our TI system, quantified by sensitivity and specificity, yielded promising results. Based on the experiments performed with 11 inclusions located at 3 different depths and having 2 different sizes and 2 different stiffness values, our TI system showed an average sensitivity of  $90.82 \pm 8.08\%$ , an average specificity of  $89.80 \pm 12.66\%$ , an average *PPV* of  $90.50 \pm 11.09\%$ , and an average *NPV* of  $90.29 \pm 9.26\%$ . The use of the proposed TI system at home is justifiable if we consider the sensitivity and specificity values reported for BSE in [15], which vary between 26-89% and 66-81%, respectively. The sensitivity and the specificity values reported for CBE are 54% and 94.0%, respectively and higher than that of BSE [54]. Mammography demonstrates a sensitivity of 70% and a specificity of 92% [55]. MRI shows a sensitivity of 87.5% and a specificity of 92.8% in high risk women population [56-61]. Scaperrotta et al. [62] evaluated 293 breast lesions with B-mode ultrasound and UE. They reported the sensitivity and the specificity of UE as 80% and 80.9%, respectively. The results showed that the performance of UE is inferior to the conventional ultrasound (95.4% sensitivity and 87.4% specificity). Raza and Baum [63] reported the sensitivity and specificity rate of the Doppler Sonography as 68% and 95%, respectively. Sinkus et al. [64] analyzed 38 malignant and 30 benign lesions with MRE and reported its sensitivity and specificity as 95% and 80%, respectively.

## 5.2.2 Comparison with the other TI systems

### 5.2.2.1 Sensitivity and specificity performance

The performance our TI system is comparable to the other TI systems. Kaufman et al. [45] examined 110 patients having breast masses and succeeded to detect 94% of these masses, while manual palpation could detect 86% of them. Egorov et al. [65] reported the sensitivity and the specificity of their TI system as 89.4 % and 88.9% with standard deviations of  $\pm 7.8\%$  and  $\pm 7.6\%$ , respectively, based on the experiments performed on 154 benign and 33 malignant lesions. Yegingil [66] reported the sensitivity and specificity of their device to invasive carcinoma as 89% and 82%, respectively. Also, the malignancy of a tumor was predicted with 96% sensitivity and 54% specificity [66-68].

### 5.2.2.2 Inclusion detection performance

The results of the compression experiments showed that the proposed TI system successfully detected all the tumor-like inclusions embedded into a tissue-like silicon sample. This was achieved by comparing the measured data with the reference (i.e. control) data collected from an empty sample. In our experiments, the most challenging inclusion had a diameter of 10 mm and was located at 20 mm in depth. The inclusion detection capability of the other TI systems is compatible to ours. Egorov et al. [44] prepared a silicon model containing inclusions with 6, 8, 11, 14.5 mm in diameters. These inclusions were embedded into the model at the varying depths of 7.5-35 mm. The elastic modulus of the silicon model and the inclusions were 8 kPa and 175 kPa, respectively. They successfully detected inclusions, having a diameter of 11 mm diameter, up to 20 mm in depth using the Max/Base > noise criterion and also up to 27.5 mm in depth using an estimation algorithm based on neural networks. In addition, smaller inclusions having 6 mm diameter were detected up to 10 mm in depth using Max/Base > noise criterion and up to 17.5 mm in depth using the neural networks. The

---

stiffness of their inclusions was about 22 times stiffer than that of the silicon sample. Wellman et al. [47] conducted experiments with 23 women subject who underwent breast surgery. Before the surgery, the size of each breast mass was estimated by their TI system utilizing an array of pressure sensors. Their TI system estimated the size of the breast masses with a mean absolute error of 13% while the CBE and ultrasonography yielded the mean errors in size of 46% and 34%, respectively. Yegingil [66] used a gelatin model with silicon inclusions located at depths varying between 1-17 mm. The inclusions were 38 times stiffer than the gelatin model. They successfully detected the silicon inclusions located up to 8, 12, and 17 mm using three piezoelectric finger having different shape, size, and sensitivity. Omata et al. [50] prepared a silicone rubber phantom and silicone inclusions with 13 mm in diameter and in three different elastic moduli: 25, 62, and 254 kPa. The depths of the inclusions from the top surface of the silicon phantom varied from 4 to 20 mm. The results of the experiments showed that the TI system could detect inclusions up to 20 mm in depth. Here, it is important to emphasize that the stiffness contrast between the silicone phantom and the tumor-like inclusions used in all of the above studies is higher than that of ours, which makes easier it for their devices to detect the inclusions.



## Chapter 6

### 6. CONCLUSION AND FUTURE WORK

The aim of this study was to develop a low-cost TI system, which can be used by clinicians and home users to detect tumors in breast tissue. Our initial goal was to develop a prototype system that performs as good as manual palpation (in fact, the experiments performed with silicon samples showed that the proposed system performed better in detecting deep inclusions than manual palpation) while providing quantitative and objective data to the user. Having a TI system at home, returning quantitative data, is important for the cancer patients not only for the reasons of privacy and personal comfort, but also to record and monitor their progress regularly. Moreover, if the information recorded by the proposed TI system can be transferred to the hospital over the internet, the response of the patients to a new treatment method or a drug can be analyzed more thoroughly.

In the future, we would like to conduct clinical studies and test our TI system on patients having breast cancer to compare its performance with the conventional devices and methods. For this purpose, we plan to miniaturize our system and increase the number of sensors per area. Furthermore, we will integrate an embedded position tracking system into our design to measure the compression depth of the tactile sensor into the breast tissue. The position tracking system will enhance the mobility of the system while enabling the hand-held use of the proposed TI system. Also, the palpation procedure needs to be standardized for the clinical experiments. Moreover, plastic round tips will be attached to the metal contour pins used in the current design to make the use of device more comfortable for the patients. Finally, the software developed for

detecting inclusions from tactile images can be improved by implementing more advanced statistical estimation methods as suggested in other breast imaging studies.

---

## REFERENCES

- [1] Ferlay, J., Shin, H. R., Bray, F., Forman, D., Mathers, C., and Parkin, D. M., "Estimates of Worldwide Burden of Cancer in 2008: Globocan 2008," *International Journal of Cancer*, vol. 127, no.12, pp. 2893-291, June 2010.
- [2] Khatib, O. M. N., "*Guidelines for the Prevention, Management and Care of Diabetes Mellitus*," Who Emro Technical Publication, WHO Regional Office for the Eastern Mediterranean, Cairo, 2006.
- [3] Hermanek, P., Sobin, L. H., and International Union against Cancer, *Tnm Classification of Malignant Tumours*, Uicc International Union against Cancer, 7<sup>th</sup> ed. New York: Springer-Verlag, 1987.
- [4] Sarvazyan, A., Egorov, V., Son, J. S., and Kaufman, C. S., "Cost-Effective Screening for Breast Cancer Worldwide: Current State and Future Directions," *Breast Cancer: Basic and Clinical Research*, vol. 1, pp. 91-99, July 2008.
- [5] National Cancer Institute, "Male Breast Cancer Treatment," <http://www.cancer.gov/cancertopics/pdq/treatment/malebreast/HealthProfessional>, 2011.
- [6] International Agency for Research on Cancer, "World Cancer Report," [http://www.iarc.fr/en/publications/pdfs-online/wcr/2008/wcr\\_2008.pdf](http://www.iarc.fr/en/publications/pdfs-online/wcr/2008/wcr_2008.pdf), 2008.
- [7] Ries Lag, Melbert D., Krapcho M., Mariotto A., Miller B. A., Feuer E. J., Clegg L., Horner M. J., Howlader N., Eisner M. P., Reichman M., and K, E. B., "Seer Cancer Statistics Review," [http://seer.cancer.gov/csr/1975\\_2004/](http://seer.cancer.gov/csr/1975_2004/), 2007.
- [8] Slowik, G., "Breast Cancer," <http://ehealthmd.com/library/breastcancer>, 2011.
- [9] Sariago, J., "Breast Cancer in the Young Patient," *The Amerikan Surgeon*, vol. 76, no. 12, pp. 1397-1400, 2010.
- [10] Chang, L., "Benign Breast Lumps", <http://www.webmd.com/breast-cancer/benign-breast-lumps>, 2009.
- [11] Maclean, J., "Breast Cancer in California: A Closer Look," *California Breast Cancer Research Program*, pp. 22-24, 2004.
- [12] Nover, A. B., Jagtap, S., Anjum, W., Yegingil, H., Shih, W. Y., Shih, W. H., and Brooks, A. D., "Modern Breast Cancer Detection: A Technological Review," *International Journal of Biomedical Imaging*, vol. 902326, September 2009.
- [13] Lang, P., "Introduction Optical Tactile Sensors for Medical Palpation," in *Proc. The Thirty-Fourth London District Science and Technology Conference*, pp. 1-5, March 2004.
- [14] Vahabi, M., "Breast Cancer Screening Methods: A Review of the Evidence," *Health Care for Women International*, vol. 24, no. 9, pp. 773-793, 2003.
- [15] Kusters, J. P., and Gotzsche, P. C., "Regular Self-Examination or Clinical Examination for Early Detection of Breast Cancer," *Cochrane Database of Systematic Reviews*, vol. 2, no. CD003373, 2003.
- [16] Semiglazov, V. F., Sagaidak, V. N., Moiseyenko, V. M., and Mikhailov, E. A., "Study of the Role of Breast Self-Examination in the Reduction of Mortality from Breast-Cancer," *European Journal of Cancer*, vol. 29A, no.14, pp. 2039-2046, 1993.
- [17] Thomas, D. B., Gao, D. L., Ray, R. M., Wang, W. W., Allison, C. J., Chen, F. L., Porter, P., Hu, Y. W., Zhao, G. L., Pan, L. D., Li, W. J., Wu, C. Y., Coriaty, Z., Evans, I., Lin, M. G., Stalsberg, H., and Self, S. G., "Randomized Trial of Breast Self-Examination in

- Shanghai: Final Results," *Journal of the National Cancer Institute*, vol. 94, no. 19, pp. 1445-1457, 2002.
- [18] American Cancer Society, "Breast Cancer Facts and Figures 2007-2008", *American Cancer Society*, Atlanta, Technical Report, 2008.
- [19] Pilgrim, C., Lannon, C., Harris, R. P., Cogburn, W., and Fletcher, S. W., "Improving Clinical Breast Examination Training in a Medical School: A Randomized Controlled Trial," *Journal of General Internal Medicine*, vol. 8, no. 2, pp. 685-688, 1993.
- [20] Wiecha, J. M., and Gann, P., "Provider Confidence in Breast Examination," *Family Practice Research Journal*, vol. 13, no. 1, pp. 37-41, 1993.
- [21] Lane, D. S., and Burg, M. A., "Promoting Physician Preventive Practices: Needs Assessment for Cme in Breast Cancer Detection," *Journal of Continuing Education in the Health Professions*, vol. 9, no. 4, pp. 245-56, 1989.
- [22] Oestreicher, N., White, E., Lehman, C. D., Mandelson, M. T., Porter, P. L., and Taplin, S. H., "Predictors of Sensitivity of Clinical Breast Examination (Cbe)," *Breast Cancer Research and Treatment*, vol. 76, no. 1, pp. 73-81, 2002.
- [23] Bancej, C., Decker, K., Chiarelli, A., Harrison, M., Turner, D., and Brisson, J., "Contribution of Clinical Breast Examination to Mammography Screening in the Early Detection of Breast Cancer," *Journal of Medical Screening*, vol. 10, no. 1, pp. 16-21, 2003.
- [24] Brown, M. L., Goldie, S. J., Draisma, G., Harford, J., and Lipscomb, J., "*Disease Control Priorities in Developing Countries*," chapter 29, 2<sup>nd</sup> edition, 2006.
- [25] Zeng, J., Wang, Y., Freedman, M., and Mun, S. K., "Finger Tracking for Breast Palpation Quantification with Stereo Color Cameras," [http://www.simulation.georgetown.edu/spie\\_oe.html](http://www.simulation.georgetown.edu/spie_oe.html), 2002.
- [26] Armstrong, K., Moye, E., Williams, S., Berlin, J. A., and Reynolds, E. E., "Screening Mammography in Women 40 to 49 Years of Age: A Systematic Review for the American College of Physicians," *Annals of Internal Medicine*, vol. 146, no. 7, pp. 516-526, 2007.
- [27] Howe, G. R., and Mclaughlin, J., "Breast Cancer Mortality between 1950 and 1987 after Exposure to Fractionated Moderate-Dose-Rate Ionizing Radiation in the Canadian Fluoroscopy Cohort Study and a Comparison with Breast Cancer Mortality in the Atomic Bomb Survivors Study," *Radiation Research*, vol. 145, no. 6, pp. 694-707, 1996.
- [28] Uchida, K., Yamashita, A., Kawase, K., and Kamiya, K., "Screening Ultrasonography Revealed 15% of Mammographically Occult Breast Cancers," *Breast Cancer*, vol. 15, no. 2, pp. 165-168, 2008.
- [29] Kolb, T. M., Lichy, J., and Newhouse, J. H., "Occult Cancer in Women with Dense Breasts: Detection with Screening Us- Diagnostic Yield and Tumor Characteristics," *Radiology*, vol. 207, no. 1, pp. 191-199, 1998.
- [30] Squire, L., and Novelline, R., *Squire's Fundamentals of Radiology*, Harvard University Press, 5<sup>th</sup> ed., 1997.
- [31] Orel, S. G., and Schnall, M. D., "Mr Imaging of the Breast for the Detection, Diagnosis, and Staging of Breast Cancer," *Radiology*, vol. 220, no. 1, pp. 13-30, 2001.
- [32] Cancerhelp Uk, Mri Scan, <http://www.cancerhelp.org.uk/about-cancer/tests/mri-scan>, 2011.
- [33] Imaginis, "Scientists Find Mammography Is Still "Gold Standard" for Breast Cancer Detection but Recommend Research into More Accurate Methods," <http://www.imaginis.com/breast-health-news/scientists-find-mammography-is-still-quot-gold-standard-quot-for-breast-cancer-detection-but-recomme>, 2001.

- [34] Sehgal, C. M., Weinstein, S. P., Arger, P. H., and Conant, E. F., "A Review of Breast Ultrasound," *Journal of Mammary Gland Biology and Neoplasia*, vol. 11, no. 2, pp. 113-23, 2006.
- [35] Nemecek, C. F., Listinsky, J., and Rim, A., "How Should We Screen for Breast Cancer? Mammography, Ultrasonography, Mri," *Cleveland Clinic Journal of Medicine*, vol. 74, no. 12, pp. 897-904, 2007.
- [36] Cosgrove, D. O., Kedar, R. P., Bamber, J. C., Al-Murrani, B., Davey, J. B., Fisher, C., Mckinna, J. A., Svensson, W. E., Tohno, E., Vagios, E., and Et Al., "Breast Diseases: Color Doppler Us in Differential Diagnosis," *Radiology*, vol. 189, no.1, pp. 99-104, 1993.
- [37] Mcknight, A. L., Kugel, J. L., Rossman, P. J., Manduca, A., Hartmann, L. C., and Ehman, R. L., "Mr Elastography of Breast Cancer: Preliminary Results," *American Journal of Roentgenology*, vol. 178, no. 6, pp. 1411-1417, 2002.
- [38] Samani, A., Bishop, J., Luginbuhl, C., and Plewes, D. B., "Measuring the Elastic Modulus of Ex Vivo Small Tissue Samples," *Physics in Medicine and Biology*, vol. 48, no. 14, pp. 2183-2198, 2003.
- [39] Wellman, P. S., Howe, R. D., Dalton, E., and Kern, K. A., "Breast Tissue Stiffness in Compression Is Correlated to Histological Diagnosis," <http://biorobotics.harvard.edu/pubs/1999/mechprops.pdf>, 1999.
- [40] Sarvazyan, A., Goukassian, D., Maevsky E, and G, O., "Elasticity Imaging as a New Modality of Medical Imaging for Cancer Detection," *Computer-Based Medical Systems, Proceedings of the Eighth IEEE Symposium*, pp. 69–81, 1995.
- [41] Skovorda, A. R., Klishko, A. N., Gusakian, D. A., Maevskii, E. I., Ermilova, V. D., Oranskaia, G. A., and Sarvazian, A. P., "Quantitative Analysis of Mechanical Characteristics of Pathologically Altered Soft Biological Tissues," *Biofizika*, vol. 40, no. 6, pp. 1335-1340, 1995.
- [42] Krouskop, T. A., Wheeler, T. M., Kallel, F., Garra, B. S., and Hall, T., "Elastic Moduli of Breast and Prostate Tissues under Compression," *Ultrasonic Imaging*, vol. 20, no. 4, pp. 260-274, 1998.
- [43] "Medical Tactile Inc. Los Angeles Ca, Suretouch," <http://www.medicaltactile.com>.
- [44] Egorov, V., and Sarvazyan, A. P., "Mechanical Imaging of the Breast," *IEEE Transactions on Medical Imaging*, vol. 27, no. 9, pp. 1275-1287, 2008.
- [45] Kaufman, C. S., Jacobson, L., Bachman, B. A., and Kaufman, L. B., "Digital Documentation of the Physical Examination: Moving the Clinical Breast Exam to the Electronic Medical Record," *The American Journal of Surgery*, vol. 192, no. 4, pp. 444-449, 2006.
- [46] "Assurance Medical Corp., Breast View System," [www.assurancemed.com](http://www.assurancemed.com).
- [47] Wellman, P. S., Dalton, E. P., Krag, D., Kern, K. A., and Howe, R. D., "Tactile Imaging of Breast Masses: First Clinical Report," *Archives of Surgery*, vol. 136, no. 2, pp. 204-208, 2001.
- [48] Wellman, P. S., and Howe, R. D., "Extracting Features from Tactile Maps," in *Proc. Medical Image Computing and Computer-Assisted Intervention*, vol. 1679, pp. 1133-1142, 1999.
- [49] Yegingil, H. O., Shih, W. Y., Anjum, W., Brooks, A. D., and Shih, W. H., "Soft Tissue Elastic Modulus Measurement and Tumor Detection Using Piezoelectric Fingers," *Materials Research Society*, vol. 898, pp. 1-6, 2005.
- [50] Omata, S., Murayama, Y., Haruta, M., Hatakeyama, Y., Shiina, T., Sakuma, H., Takenoshita, S., and Constantinou, C. E., "Development of a New Instrument for

- Examination of Stiffness in the Breast Using Haptic Sensor Technology," *Sensors and Actuators A: Physical*, vol. 143, no. 2, pp. 430-438, 2008.
- [51] Ayyildiz, M., Guclu, B., Yildiz, M. Z., and Basdogan, C., "A Novel Tactile Sensor for Detecting Lumps in Breast Tissue," in *Proc. International Conference on Eurohaptics, Amsterdam, Netherlands, Part I*, pp. 367-372, 2010.
- [52] Ocal, S., Ozcan, M. U., Basdogan, I., and Basdogan, C., "Effect of Preservation Period on the Viscoelastic Material Properties of Soft Tissues with Implications for Liver Transplantation," *Journal of Biomechanical Engineering*, vol. 132, no. 101007, pp. 1-7, 2010.
- [53] Guclu, B., "Maximizing the Entropy of Histogram Bar Heights to Explore Neural Activity: A Simulation Study on Auditory and Tactile Fibers," *Acta Neurobiologiae Experimentalis (Wars)*, vol. 65, no. 4, pp. 399-407, 2005.
- [54] Barton, M. B., Harris, R., and Fletcher, S. W., "Does This Patient Have Breast Cancer? The Screening Clinical Breast Examination: Should It Be Done? How?," *Jama-Journal of the American Medical Association*, vol. 282, no. 13, pp. 1270-1280, 1999.
- [55] Pisano, E. D., Gatsonis, C., Hendrick, E., Yaffe, M., Baum, J. K., Acharyya, S., Conant, E. F., Fajardo, L. L., Bassett, L., D'orsi, C., Jong, R., and Rebner, M., "Diagnostic Performance of Digital Versus Film Mammography for Breast-Cancer Screening," *The New England Journal of Medicine*, vol. 353, no. 17, pp. 1773-1783, 2005.
- [56] Kriege, M., Brekelmans, C. T. M., Boetes, C., Besnard, P. E., Zonderland, H. M., Obdeijn, I. M., Manoliu, R. A., Kok, T., Peterse, H., Tilanus-Linthorst, M. M. A., Muller, S. H., Meijer, S., Oosterwijk, J. C., Beex, L. V. a. M., Tollenaar, R. a. E. M., De Koning, H. J., Rutgers, E. J. T., Klijin, J. G. M., and Screeni, M. R. I., "Efficacy of Mri and Mammography for Breast-Cancer Screening in Women with a Familial or Genetic Predisposition," *The New England Journal of Medicine*, vol. 351, no. 5, pp. 427-437, 2004.
- [57] Leach, M. O., Boggis, C. R. M., Dixon, A. K., Easton, D. F., Eeles, R. A., Evans, D. G. R., Gilbert, F. F., Griebisch, I., Hoff, R. J. C., Kessar, P., Lakhani, S. R., Moss, S. M., Nerurkar, A., Padhani, A. R., Pointon, L. J., Thompson, D., Warren, R. M. L., and Grp, M. S., "Screening with Magnetic Resonance Imaging and Mammography of a Uk Population at High Familial Risk of Breast Cancer: A Prospective Multicentre Cohort Study (Maribs)," *Lancet*, vol. 365, no. 9473, pp. 1769-1778, 2005.
- [58] Warner, E., Plewes, D. B., Hill, K. A., Causer, P. A., Zubovits, J. T., Jong, R. A., Cutrara, M. R., Deboer, G., Yaffe, M. J., Messner, S. J., Meschino, W. S., Piron, C. A., and Narod, S. A., "Surveillance of Brca1 and Brca2 Mutation Carriers with Magnetic Resonance Imaging, Ultrasound, Mammography, and Clinical Breast Examination," *Jama-Journal of the American Medical Association*, vol. 292, no. 11, pp. 1317-1325, 2004.
- [59] Kuhl, C. K., Schrading, S., Leutner, C. C., Morakkabati-Spitz, N., Wardelmann, E., Fimmers, R., Kuhn, W., and Schild, H. H., "Mammography, Breast Ultrasound, and Magnetic Resonance Imaging for Surveillance of Women at High Familial Risk for Breast Cancer," *Journal of Clinical Oncology*, vol. 23, no. 33, pp. 8469-8476, 2005.
- [60] Lehman, C. D., Blume, J. D., Weatherall, P., Thickman, D., Hylton, N., Warner, E., Pisano, E., Schmitt, S. J., Gatsonis, C., Schnall, M., and Wor, I. B. M. C., "Screening Women at High Risk for Breast Cancer with Mammography and Magnetic Resonance Imaging," *Cancer*, vol. 103, no. 9, pp. 1898-1905, 2005.
- [61] Ely, S., and Vioral, A. N., "Breast Cancer Overview," *Plastic Surgical Nursing*, vol. 27, no. 3, pp. 128-133, 2007.

- 
- [62] Scaperrotta, G., Ferranti, C., Costa, C., Mariani, L., Marchesini, M., Suman, L., Folini, C., and Bergonzi, S., "Role of Sonoelastography in Non-Palpable Breast Lesions," *European Radiology*, vol. 18, no. 11, pp. 2381-2389, 2008.
- [63] Raza, S., and Baum, J. K., "Solid Breast Lesions: Evaluation with Power Doppler Us," *Radiology*, vol. 203, no. 1, pp. 164-168, 1997.
- [64] Sinkus, R., Siegmann, K., Tanter, M., Xydeas, T., and Fink, M., "MR Elastography of Breast Lesions: Understanding the Solid/Liquid Duality Can Improve the Specificity of Contrast-Enhanced MR Mammography", *Magnetic Resonance in Medicine*, vol. 58, pp. 1135–1144, 2007.
- [65] Egorov, V., Kearney, T., Pollak, S. B., Rohatgi, C., Sarvazyan, N., Airapetian, S., Browning, S., and Sarvazyan, A., "Differentiation of Benign and Malignant Breast Lesions by Mechanical Imaging," *Breast Cancer Research and Treatment*, vol. 118, no. 1, pp. 67-80, 2009.
- [66] Yegingil, H. O., 2009, "Breast Cancer Detection and Differentiation Using Piezoelectric Fingers," Ph.D.dissertation, *Drexel University, School of Biomedical Engineering*, 2009.
- [67] Yegingil, H., Shih, W. Y., and Shih, W. H., "All-Electrical Indentation Shear Modulus and Elastic Modulus Measurement Using a Piezoelectric Cantilever with a Tip," *Journal of Applied Physics*, vol. 101, no. 5, pp. 054510 - 054510-10, March 2007.
- [68] Yegingil, H., Shih, W. Y., and Shih, W. H., "Probing Elastic Modulus and Depth of Bottom-Supported Inclusions in Model Tissues Using Piezoelectric Cantilevers," *Review of Scientific Instruments*, vol. 78, no. 11, pp. 115101 - 115101-6, November 2007.